The *JNM1* Gene in the Yeast *Saccharomyces cerevisiae* Is Required for Nuclear Migration and Spindle Orientation During the Mitotic Cell Cycle

John N. McMillan and Kelly Tatchell

Department of Microbiology, North Carolina State University, Raleigh, North Carolina 27695

Abstract. *JNM1*, a novel gene on chromosome XIII in the yeast *Saccharomyces cerevisiae*, is required for proper nuclear migration. *jnm1* null mutants have a temperature-dependent defect in nuclear migration and an accompanying alteration in astral microtubules. At 30°C, a significant proportion of the mitotic spindles is not properly located at the neck between the mother cell and the bud. This defect is more severe at low temperature. At 11°C, 60% of the cells accumulate with large buds, most of which have two DAPI staining regions in the mother cell. Although mitosis is delayed and nuclear migration is defective in *jnm1* mutants, we rarely observe more than two nuclei in a cell, nor do we frequently observe anuclear cells. No loss of viability is observed at 11°C and cells continue to grow exponentially with increased doubling time. At low temperature the large budded cells of *jnm1* mutants exhibit extremely long astral microtubules that often wind around the periphery of the cell. *jnm1* mutants are not defective in chromosome segregation during mitosis, as assayed by the rate of chromosome loss, or nuclear migration during conjugation, as assayed by the rate of mating and cytoduction. The phenotype of a *jnm1* mutant is strikingly similar to that for mutants in the dynein heavy chain gene (Eshel, D., L. A. Urrestarazu, S. Vissers, J.-C. Jauniaux, J. C. van Vliet-Reedijk, R. J. Plants, and I. R. Gibbons. 1993. *Proc. Natl. Acad. Sci. USA.* 90:11172–11176; Li, Y. Y., E. Yeh, T. Hays, and K. Bloom. 1993. *Proc. Natl. Acad. Sci. USA.* 90:10096–10100). The *JNM1* gene product is predicted to encode a 44-kD protein containing three coiled coil domains. A *JNM1:lacZ* gene fusion is able to complement the cold sensitivity and microtubule phenotype of a *jnm1* deletion strain. This hybrid protein localizes to a single spot in the cell, most often near the spindle pole body in unbudded cells and in the bud in large budded cells. Together these results point to a specific role for Jnm1p in spindle migration, possibly as a subunit or accessory protein for yeast dynein.

THE nuclei in the budding yeast *Saccharomyces cerevisiae* migrate to the neck between the mother cell and the bud prior to mitosis and the spindle microtubules orient along the long axis of the cell. At mitosis the spindle elongates through the neck between the mother cell and the bud and chromosomes separate, depositing one set of chromosomes in the mother cell body and one set in the bud. A key role for microtubules in this process has been shown by the inhibitory effects on nuclear migration by microtubule inhibitors (Jacobs et al., 1988) and by defects in nuclear migration exhibited by some β tubulin mutants (Huffaker et al., 1988). Cytoplasmic (or astral) microtubules appear to be mainly responsible for nuclear migration. Mutant alleles of the *tub2* gene that impart a specific defect in astral microtubule stability show defects in nuclear migration during mitosis or karyogamy, but have relatively little effect on mitosis (Palmer et al., 1992; Sullivan and Huffaker, 1992). In contrast, β tubulin mutations that do not affect astral microtubules are able to carry out nuclear fusion during karyogamy and nuclear migration during the mitotic cell cycle (Huffaker et al., 1988).

The essential role of astral fibers in spindle orientation and nuclear migration suggests that the nucleus is pulled or pushed to the bud neck by astral fibers. If this model is correct, two fundamental questions remain. First, what force-generating system or systems are required to move the spindle to the bud neck? Second, what molecules tether the astral fibers in order for force to be exerted? Palmer et al. (1992) suggested that actin may play a role in tethering microtubules. They have shown that disruption of actin function by shifting a temperature-sensitive actin mutant to the nonpermissive temperature causes misorientation of spindles and subsequent production of binucleate cells. The precise role for actin in nuclear migration is not known, but a likely possibility is that actin may have a role in tethering astral microtubules to sites in the bud (Palmer et al., 1992).

Address all correspondence to Kelly Tatchell, Department of Microbiology, Box 7615, North Carolina State University, Raleigh, NC 27695.

Recently, five kinesin-like genes, *KAR3* (Meluh and Rose, 1990), *CIN8* (Hoyt et al., 1992; Roof et al., 1992), *KIP1* (Hoyt et al., 1992; Roof et al., 1992) *KIP2* (Roof et al., 1992), and *SMY1* (Lillie and Brown, 1992), have been identified in budding yeast. Some of these play important roles in spindle function but there is no evidence that their gene products are required for nuclear migration during the mitotic cell cycle. *KAR3* is required for nuclear migration during karyogamy (Meluh and Rose, 1990) but is not required for nuclear migration during mitosis (cited in Palmer et al., 1992). A dynein heavy chain gene in yeast, *DHC1/DYN1*, has recently been reported (Eshel et al., 1993; Li et al., 1993) whose product may have a role in nuclear migration. A disruption of the *DHC1* gene results in a defect in spindle orientation and nuclear migration. *dhc1* mutants show a significant fraction of large budded cells that contain two nuclear staining regions and a single misoriented spindle. This defect is more severe at low temperature. Nevertheless, *dhc1* mutants grow with only slightly increased doubling times at 30°C, indicating that Dhc1p function is either duplicated in yeast or is possibly redundant with another motor system. Although cytoplasmic dynein has been implicated in chromosome segregation in mammalian systems (Pfarr et al., 1990; Steuer et al., 1990), *dhc1* mutants exhibit no defects in chromosome loss or mating (Li et al., 1993).

Other mutants have been identified that also exhibit a nuclear migration defect (Watts et al., 1987; Berlin et al., 1990; Kormanec et al., 1991; Ursic and Culbertson, 1991; McConnell and Yaffe, 1992). The specific role of these genes in nuclear migration is not known and in all cases except *num1* the nuclear migration defect is only one trait of a more complex phenotype.

In this paper we describe the characterization of a yeast mutant, named *JNM1* for just nuclear migration, that has a remarkably similar phenotype to that of *dhc1/dyn1*. *jnm1* null mutants are viable and exhibit normal rates of chromosome loss during mitosis and nuclear fusion during mating, but have a defect in nuclear migration that is exacerbated at low temperature.

Materials and Methods

Reagents

Fluorescent Brightener 28 (calcofluor), thiabendazole (TBZ),[1] and FITC-labeled goat anti-rat IgG antibody were purchased from Sigma Chemical Co., St. Louis, MO. Calcofluor was stored as a 1 mg/ml stock solution in dH_2O (4°C) and TBZ as a 40 mg/ml stock solution dissolved in dimethylsulfoxide (−20°C). 4',6'-diamidino-2-phenylindole (DAPI), β-Glucuronidase/Arylsulfatase, and TRITC-labeled goat anti-rabbit IgG antibody were purchased from Boehringer Mannheim Corp., Indianapolis, IN. DAPI was stored at 4°C as a 1 mg/ml stock solution in dH_2O. The anti-tubulin YOL1/34 monoclonal antibody was purchased from Accurate Chemical and Scientific Corp., Westbury, NY. The rabbit anti-β-galactosidase polyclonal antibody was purchased from Organon Teknika Corp., Rockville, MD. FITC-labeled goat anti-mouse IgG antibody was purchased from Jackson ImmunoResearch Labs, Inc., Nest Grove, PA. The anti-tubulin 4A1 monoclonal antibody was a generous gift from John Cooper (Washington University, St. Louis, MO). Benomyl was a generous gift from Andy Hoyt (Johns Hopkins University, Baltimore, MD) and stored as a 20 mg/ml stock solution dissolved in dimethylsulfoxide.

1. *Abbreviations used in this paper*: cM, centimorgans; cyh, cycloheximide; DAPI, 4',6'-Diamidino-2-phenylindole; SPB, spindle pole body; TBZ, thiabendazole.

Media, Yeast Strains, Plasmids, and Construction of Deletion Mutations

Rich medium (YPD) contained 1% yeast extract, 2% peptone, and 2% glucose. YPG + cyh medium contained 1% yeast extract, 2% peptone, 3% (vol/vol) glycerol, and 10 μg/ml cycloheximide (cyh). Minimal, synthetic complete, and drop-out media have been described (Rose et al., 1990). Benomyl, TBZ, and EtBr were added to YPD just prior to pouring plates. Cells were induced to sporulate on medium containing 1% yeast extract, 2% peptone, and 2% acetate.

Yeast strains with genotypes and origins are shown in Table I. *jnm1* was uncovered in the temperature-sensitive strain SC3B. Strain 26218B is a *jnm1-1* spore clone isolated from a cross of JC530-4B and SC3B. Strains JM100 and 26B are *jnm1-1* spore clones isolated from crosses of 26218B and 246.1.1 with RW2401, respectively. The *jnm1-1* mutation in 26B was serially backcrossed eight times to JC482, obtaining strains JM116 and JM117. The null mutations, *jnm1-Δ1*, *jnm1-Δ2*, and *jnm1-Δ3*, were introduced into strains by one-step gene replacement (Rothstein, 1983). *rho°* strains were isolated by growing cells in minimal broth medium plus the addition of any required amino acids or pyrimidine bases and 25 μg/ml ethidium bromide as described (Goldring et al., 1970). *rho°* isolates were confirmed by their inability to grow on nonfermentable carbon sources and by DAPI staining of the cells. cyh^r strains were isolated by spontaneous reversion to cyh resistance on synthetic complete medium plus 3 μg/ml cyh.

pJM1325 was constructed by inserting the 3.2-kb BamHI fragment containing the *JNM1* open reading frame from plasmid pJM1312, one of the original library clone isolates (see below), into the BamHI site of YEp352. Plasmids pJM1435-pJM1454 are a series of ExoIII deletions of the 3.2-kb BamHI fragment inserted into the BamHI site of the centromere-based vector pUN55 (Elledge and Davis, 1988). The inserts are derived from the same ExoIII deletion series constructed in plasmid pJM1329 for the purpose of sequencing (see below). pJM1470 was constructed by placing an EcoRI site at the 3' end of the *JNM1* ORF with PCR using the oligonucleotide 5'-TCCGCGAATTCTTTGCTATTTCTCTGTAGAG-3', resulting in the replacement of the putative *JNM1* stop codon TAA with GAA encoding glutamic acid. The BamHI/EcoRI fragment containing the *JNM1* ORF was ligated into the BamHI/EcoRI site of YIp356R (Myers et al., 1986) creating an in-frame fusion with the *E. coli lacZ* gene. To integrate this *JNM1-lacZ* fusion at the *JNM1* chromosomal locus, this plasmid, pJM1470, was linearized with SpeI and transformed into strain JM140.

The null allele *jnm1-Δ1* was constructed by piecing together upstream and downstream regions of the *JNM1* open reading frame (ORF) into the pBLUESCRIPT SK⁻ (Strategene Cloning Systems, La Jolla, CA) polylinker cloning site. Using PCR, an EcoRI site was placed 10 nucleotides upstream of the putative *JNM1* start codon and this 1.2-kb ClaI/EcoRI fragment was ligated into the pBLUESCRIPT vector. Likewise, the 0.6-kb NdeI/XbaI fragment, located just 3' of the *JNM1* ORF, was placed into this construct in the correct orientation relative to the upstream 1.2-kb fragment. A 2.0-kb HpaI/SalI *LEU2* fragment was blunt end ligated into the EcoRI site. This construct deleted the entire *JNM1* ORF, replacing it with the yeast *LEU2* gene (Fig. 1 *C*). The *jnm1-Δ2* allele was constructed by deleting two adjacent HindIII fragments (345 nucleotides) within the *JNM1* ORF and inserting a 1.2-kb HindIII fragment containing the yeast *URA3* gene. The *jnm1-Δ3* allele was constructed in the same manner as the *jnm1-Δ2* allele, except a 2.0-kb HpaI/SalI *LEU2* fragment was blunt end ligated into the blunt ended HindIII sites (Fig. 1 *C*). 5' overhangs were filled in with Klenow enzyme (New England Biolabs, Inc., Beverly, MA) when necessary for blunt end ligations.

DNA Manipulations

Yeast cells were transformed by electroporation (Becker and Guarente, 1991) or by the LiAc procedure (Ito et al., 1983; Gietz et al., 1992). The generation of nested sets of deletions with ExoIII has been described (Sambrook et al., 1989).

Cloning and Sequence Analysis of JNM1

JM100 was transformed with two YCp50 libraries kindly provided by Doug Conklin (University of Wisconsin, Madison, WI) and Leo Parks (North Carolina State University, Raleigh, NC) and with a YEp352 library (Doug Conklin). These libraries were introduced into JM100 by electroporation and immediately plated onto Ura dropout + 1 M sorbitol medium and incubated at 38°C. After growth, colonies were replica plated onto Ura dropout medium and again incubated at 38°C. Plasmids from colonies able to

Table I. Yeast Strains

Strain	Genotype	Source or Reference
SC3B	*MATα ura3-52 ade2-101 leu2 his3 ins1^{ts}*	Mike Engler (The University of Texas Health Sciences Center, Houston TX)
26218B	*MATa ura3 leu2 jnm1-1*	This study
RW2401	*MATα ura3 leu2 Δtrp1 his4 lys2 srkl::URA3*	Joann Gaughran (North Carolina State University, Raleigh, NC)
26B	*MATα ura3 leu2 trp1 lys2 jnm1-1*	This study
JM100	*MATα ura3 leu2 trp1 jnm1-1*	This study
JM103*	*MATa ura3-52 his4 JNM1* tagged with *URA3*	This study
JM127*	*MATα ura3-52 leu2 his4 jnm1-Δ1*	This study
JM115*	*MATa ura3-52 leu2 his4 jnm1-Δ2*	This study
JM118*	*MATα ura3-52 leu2 his4 jnm1-Δ2*	This study
JM154	*MATa ura3-52 can1-100 ADE4 SUP8* *MATα ura3-52 can1-100 ade4 sup8 jnm1-Δ2*	This study
JC482*	*MATα ura3-52 leu2 his4*	(Cannon and Tatchell, 1987)
JC530-4B*	*MATa ura3-52 leu2 his4*	John Cannon (University of Missouri, Columbia, MO)
JM132*	*MATa ura3-52 leu2 his4 jnm1-Δ2* *MATα ura3-52 leu2 his4 JNM1*	This study
JM116‡	*MATa ura3-52 leu2 his4 jnm1-1*	This study
JM117‡	*MATα ura3-52 leu2 his4 jnm1-1*	This study
JM120*	*MATα ura3-52 leu2 his4 rho°*	This study
JM121*	*MATa ura3-52 leu2 his4 rho°*	This study
JM122*	*MATa ura3-52 leu2 his4 jnm1-Δ2 rho°*	This study
JM123*	*MATα ura3-52 leu2 his4 jnm1-Δ2 rho°*	This study
KT1113§	*MATα ura3-52 leu2 his3*	This study
JM126‖	*MATα ura3-52 leu2 his3 jnm1-Δ2*	This study
JM150*	*MATa ura3-52 leu2 his4 cyh^r* rho°	This study
JM151*	*MATa ura3-52 leu2 his4 jnm1-Δ2 cyh^r rho°*	This study
JM181‡	*MATa ura3-52 leu2 his3 jnm1-Δ1 JNM1:lacZ* *MATα ura3-52 leu2 his3 jnm1-Δ1 JNM1:lacZ*	This study
JM183‡	*MATa ura3-52 leu2 his3* *MATα ura3-52 leu2 his3*	This study
JM152*	*MATa ura3-52 leu2 his4* *MATα ura3-52 leu2 his4*	This study
JM153*	*MATa ura3-52 leu2 his4 jnm1-Δ2* *MATα ura3-52 leu2 his4 jnm1-Δ2*	This study
KT81	*MATα hom3 ilv1*	This study
JM140*	*MATa ura3-52 leu2 his4 jnm1-Δ1 rho°*	This study
JM142*	*MATa ura3-52 leu2 his4 jnm1-Δ1 JNM1:lacZ rho°*	This study

* These strains are congenic.
‡ These strains were serially backcrossed eight times into a JC482 background.
§ This strain was serially backcrossed six times into a JC482 background.
‖ This strain was serially backcrossed seven times into a JC482 background.

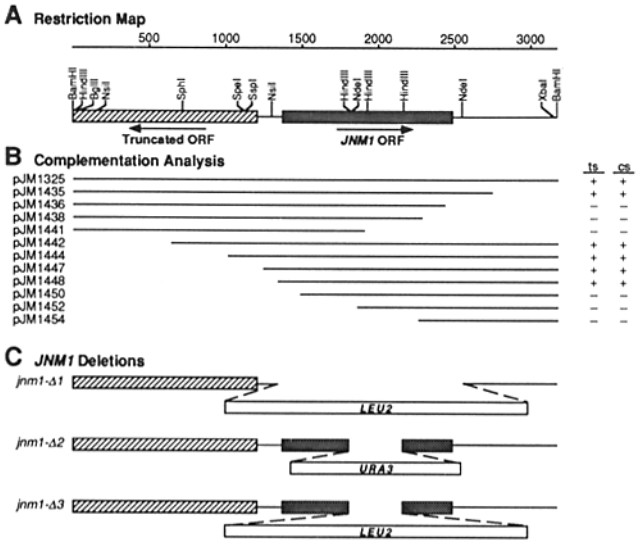

grow during the second round of incubation at 38°C were recovered and transformed into *E. coli* strain DH5αF′ (GIBCO BRL, Gaithersburg, MD). pJM1312, one of the original library clones isolated from the Doug Conklin YCp50 library, had the smallest insert, ~5.2 kb. A 3.2-kb BamHI fragment from pJM1312 that complemented *jnm1-1* was cloned into the BamHI site

Figure 1. JNM1 gene structure. (*A*) The restriction endonuclease map of the 3.2-kb BamHI fragment containing *JNM1* and flanking DNA. The shaded and hatched regions correspond to the *JNM1* open reading frame (*ORF*) and a partial open reading frame of a gene of unknown function, respectively. The arrows denote the direction of transcription on both genes, as deduced from the open reading frame. (*B*) Plasmids that contained partial deletions in the 3.2-kb BamHI fragment were transformed into a *jnm1* strain (*JM116*) and tested for their ability to complement the temperature and cold sensitivity of *jnm1*. Each horizontal bar depicts the DNA remaining in each plasmid. (*C*) The structure of a total (*jnm1-Δ1*) and partial (*jnm1-Δ2*, and *jnm1-Δ3*) *jnm1* deletions are depicted. The open regions correspond to the *LEU2* or *URA3* genes inserted into or replacing the *JNM1* locus.

of pBLUESCRIPT SK⁻ (Strategene Cloning Systems) creating pJM1329. A nested set of ExoIII deletions were constructed from both ends of the insert for sequencing. Both the template and complementary strands of the 3.2-kb insert were sequenced using a double strand template and Sequenase enzyme and reagents (Sequenase version 2.0; United States Biochemical Corp., Cleveland, OH). All sequencing reactions used the M13-20 primer or the reverse primer except for a single sequencing reaction in which a custom oligonucleotide was synthesized and used as a sequencing primer to fill an internal gap in the sequence. DNA homology searches, translation of DNA sequences, calculation of pI's, and Chou-Fasman and Robson-Garnier α-helix predictions were performed with the MacVector sequence analysis software programs (International Biotechnologies, Inc., New Haven, CT). A coiled coil prediction program (Lupas et al., 1991) was kindly supplied by Jeff Stock (Princeton University, Princeton, NJ) and run on a VAX computer using a window size of 28.

Mapping of JNM1

A Southern blot of chromosomes separated by CHEF gel electrophoresis, probed with a ^{32}P-labeled 1.8-kb HindIII fragment containing the 5′ end of the *JNM1* ORF and upstream sequence (Fig. 1 *A*), identified the *JNM1* gene as residing on chromosome XIII. The same fragment was hybridized to a set of filters (kindly supplied by Linda Riles and Maynard Olson, Washington University, St. Louis, MO) that contained an ordered set of phage λ clones representing over 80% of the yeast genome. The probe hybridized to clone 4467, which is located on chromosome XIII near *SUP8*. Tetrad analysis of JM154 revealed that *jnm1-Δ2* mapped 9.0 centimorgans (cM) from *SUP8* and 11.8 cM from *ADE4*. Spores carrying the *SUP8* allele, an ochre suppressor, were identified by their ability to suppress the ochre mutation in *can1-100*, which results in resistance to the drug canavanine. Of 229 total tetrads scored relative to the *ade4* and *jnm1* loci, there were 180 parental ditypes, 48 tetratypes, and 1 nonparental ditype. Of 227 total tetrads scored relative to the *SUP8* and *jnm1* loci, there were 186 parental ditypes, 41 tetratypes, and 0 nonparental ditypes. Distance in cM was calculated using the formula of Perkins (1949).

Growth Curves

Strains JC482 and JM118 were inoculated into YPD liquid medium and grown at 30°C. During exponential growth, 1 ml of culture was removed and inoculated into 10 ml of YPD prewarmed or prechilled to 37, 30, or 11°C. Samples of these cultures were removed at various time points, and the cells were diluted in Isoton II solution (Coulter Diagnostics, Hialeah, FL), sonicated, and cell numbers determined with a ZM Coulter Counter (Coulter Electronics, Inc., Hialeah, FL).

Immunofluorescence, DAPI, and Calcofluor Staining

rho° strains (strains lacking mitochondrial DNA) were used in DAPI staining experiments to eliminate the interference of fluorescent mitochondria. Cells were fixed for DAPI staining by adding 2 vol of ethanol directly to 1 vol of culture and incubating for 30 min at room temperature. Fixed cells were washed once with dH_2O and resuspended in 0.2 μg/ml DAPI and stored for 30 min in the dark. Cells were again washed with dH_2O and resuspended in 50% glycerol (vol/vol) and 1% β-mercaptoethanol for viewing. Cells were fixed for calcofluor/DAPI double staining as above. After fixing, cells were washed once with dH_2O and resuspended in 0.2 μg/ml DAPI. After incubating for 10 min at room temperature, 0.1 vol of a 1 mg/ml calcofluor stock solution was added and the cells were further incubated for 5 min at room temperature. Cells were then washed five times with dH_2O and resuspended in dH_2O for viewing. To visualize microtubules using the YOL1/34 anti-α tubulin primary antibody, cells were fixed for at least 2 h at room temperature in 5% formaldehyde and then treated for immunofluorescence as described (Pringle et al., 1991), using a FITC-labeled goat anti-rat IgG secondary antibody. To visualize both microtubules and the Jnm1p-β-galactosidase fusion, cells were fixed for 30 min on ice in 3.7% formaldehyde made freshly from paraformaldehyde and treated as above except that cells were incubated for 6 min in methanol (−20°C) and for 30 s in acetone (−20°C) just prior to the addition of the two primary antibodies. An anti-*Drosophila* β tubulin mouse monoclonal antibody, 4A1, and a rabbit anti-β-galactosidase polyclonal antibody were used as the primary antibodies. Under these fixation conditions we found that microtubule structures were more efficiently visualized using antibody 4A1 rather than YOL1/34. A FITC-labeled goat anti-mouse IgG antibody and a TRITC-labeled goat anti-rabbit IgG antibody were used as the secondary antibodies. DAPI was added to the mounting media or cells were incubated in DAPI just prior to the addition of the mounting media to visualize the nuclear regions. Cells were viewed and photographed with a Zeiss Axioscope microscope (Carl Zeiss, Inc., Thornwood, NY) equipped with epifluorescent and Nomarski optics.

Cell Morphology and Nuclear Position in Large Budded Cells

Strains JM120 and JM123 were grown in YPD medium at 30°C and during log phase growth 5 ml were removed and inoculated into 10 ml of YPD prewarmed to 37°C or prechilled to 11 or 13°C. After defined periods, cells were fixed and DAPI stained as above. Stained cells were spread onto a polylysine-coated slide and photographs were taken of the cells in three separate focal planes. Prints were made of the cells and the diameters of the bud and mother cell were measured using the best focal plane. Relative bud size was determined by dividing the diameter of the bud by the diameter of the mother cell. Large budded cells are defined as cells with a bud at least 2/3 the diameter of the mother cell. The percentage of cells with no buds attached was also determined. Between 133 and 192 cells were measured for each strain at each temperature. The significance of the difference in distributions of cell morphologies between JM120 and JM123 at defined temperatures was calculated using chi square analysis. Nuclear position was determined in large budded cells from the same cultures by observing where the DAPI stained regions were relative to the mother/bud neck. A large budded cell was considered to have undergone proper nuclear migration if a single DAPI staining region was lying adjacent to or in the mother/bud neck or if one DAPI staining region was in the mother cell and one in the bud. All other nuclear arrangements were considered to be abnormal. Two hundred large budded cells were analyzed for each strain at each incubation temperature and incubation time.

Localization of Anti-β-galactosidase Staining Spot in Jnm1p:β-galactosidase Cells

JNM1:lacZ cells (strains JM142 and JM181) were grown to log phase at 30°C in YPD, harvested, fixed, and stained with anti-β tubulin antibody 4A1, anti-β-galactosidase polyclonal antibody, and DAPI as described above. Nomarski, DAPI, TRITC, and FITC images of random populations of cells were photographed. The localization of the anti-β-galactosidase staining spot with respect to the spindle pole body (SPB) and astral microtubules and its position relative to the mother cell and bud were determined by analyzing the prints.

Benomyl and TBZ Sensitivity Assay

Strains JC482 and JM118 were grown to stationary phase in YPD and ~5,000 cells were placed onto YPD plates containing varying concentrations of benomyl or TBZ. These plates were incubated at 37, 24, or 13°C. Cells were allowed to grow at their respective temperatures until confluent growth was seen on control plates containing no benomyl or TBZ.

Karyogamy and Chromosome Loss Assays

Karyogamy efficiency was measured essentially as described by Rose et al. (1990). Cells were grown in YPD at 30°C and during exponential growth removed for assay. 3×10^6 cells of a *MATa rho° cyh^r his4* strain were mixed with 3×10^6 cells of a *MATα rho⁺ CYH^S his3* strain and filtered onto a 0.45-μm 25-mm filter (HAWP 025 00; Millipore Corp., Bedford, MA) using a syringe and Swinnex filter (Millipore). Filters were placed on YPD media which had been prewarmed or prechilled to 37, 30, or 13°C. Cells were incubated at 37, 30, or 13°C for 6, 4, or 10 h, respectively. After incubation the cells were washed off the filters with 1 M sorbitol and dilutions were plated onto YPG + cyh, YPD, and His⁻ Dropout media and incubated at 30°C. The mating efficiency was calculated as the percentage of diploids formed (colonies growing on His Dropout) per total number of viable cells (colonies on YPD). The cytoductant to diploid ratio was calculated as the number of cells able to grow on YPG + cyh (cytoductants) divided by the number of diploids formed. Each mating at each temperature was repeated once and averages are reported.

The rate of chromosome III loss was determined by the rate that a *MATa/MATα* diploid became mating competent. Mating competence can occur by hemizygosity or homozygosity of the *MAT* locus caused by chromosome loss or recombination, respectively. Quantitative measurement of

the mating efficiency of *MATa/MATα* diploids was determined by fluctuation analysis and calculated by the method of the median (Lea and Coulson, 1949). Diploid strains JM152 and JM153 were streaked onto YPD plates to obtain isolated colonies, and 10 colonies from each strain were inoculated into YPD liquid cultures and grown at 30°C. During exponential growth these cells were diluted in YPD and ~50 cells from each culture inoculated into 10 tubes containing 1 ml of YPD prewarmed or prechilled to 30 or 13°C or inoculated into 10 ml of YPD prewarmed to 36°C. The 1-ml cultures were allowed to grow at their respective temperatures to a density of ~1 × 10^7 cells/ml. The 10-ml 36°C cultures were grown to a lower density, ~1 × 10^6 cells/ml, because at this temperature both the wild-type and *jnm1* cells leave exponential growth at a lower density compared with cells grown at 30 or 13°C. Just prior to the mating assay, each culture was sonicated and dilutions were plated onto synthetic complete medium to determine the number of viable cells in the culture. Approximately 5 × 10^6 diploid cells, as determined by hemacytometer count, were mixed with 2 × 10^7 cells of haploid strain KT81 taken from an exponentially growing 30°C YPD culture. This cell mixture was filtered onto a 25-mm × 0.45-μm membrane (see karyogamy assay above) and incubated for 3 h at 30°C on the surface of a prewarmed YPD plate. Cells were washed from filters with dH_2O and dilutions plated onto minimal medium to select for triploids.

Results

JNM1 Is a Single Copy, Nonessential Gene and Maps to a Novel Location on Chromosome XIII

jnm1-1 was originally identified as a temperature-sensitive mutation that was partially suppressed by yeast shuttle vectors that contained the *SRK1/SSD1* gene (Wilson et al., 1991). Allelic differences in *SSD1* were found to influence the viability of strains that lacked Sit4p, a PP2A-like phosphoprotein phosphatase (Sutton et al., 1991). *SSD1*-containing plasmids were also found to partially suppress defects associated with high levels of cAMP-dependent protein kinase (Wilson et al., 1991) and deletions of the *SLK1*-encoded protein kinase (Costigan et al., 1992). The Ssd1 protein was most similar to the *dis3* gene product, a regulator of mitosis in fission yeast (Kinoshita et al., 1991). The potential role of *JNM1* in phosphoprotein metabolism prompted us to characterize this recessive mutation in detail. *jnm1-1*, originally called *ins1*, was outcrossed from strain SC3B into the strain JC482 background. We discovered that *jnm1-1* strains exhibited only a weak temperature-sensitive phenotype (*jnm1-1* strains only arrested at 38–39°C, a temperature near the upper limit for growth of our wild type strain), but they were much more sensitive to low temperature. *SRK1/SSD1*-containing plasmids had no influence on growth at low temperature (data not shown).

To clone the *JNM1* gene we transformed a *jnm1-1* strain with several yeast genomic libraries and isolated 20 plasmids that contained the same chromosomal locus (see Materials and Methods). A 3.2-kb BamHI fragment from plasmid pJM1312, one of the YCp50 library clones which complemented the temperature and cold sensitivity, was sequenced and found to contain two open reading frames oriented in opposite directions and separated by only 172 base pairs (Fig. 1 *A*). Additional subclones were constructed and tested for their ability to complement *jnm1-1*. Only those subclones that contained the open reading frame entirely within the 3.2-kb fragment were able to complement the *jnm1-1* phenotype (Fig. 1 *B*), suggesting that this open reading frame encoded the *JNM1* product.

The yeast *URA3* gene was targeted to the region of the open reading frame by homologous recombination utilizing the yeast integrating vector YIp5 and subcloned DNA from pJM1312. Tetrad analysis of a cross between the resulting Ura+ strain (JM103) and a *ura3 jnm1-1* strain (26B) revealed tight linkage between *URA3* and *jnm1-1* which argues that our clone encodes the bona fide *JNM1* gene and not an extragenic suppressor.

To determine the phenotype of a *jnm1* null mutation, a diploid heterozygous for the *jnm1-Δ1* deletion (Fig. 1 *C*) was sporulated and asci were dissected onto YPD medium. Tetrad analysis revealed that Leu+ spore clones were viable and contained an authentic deletion of the *JNM1* gene as determined by Southern blot analysis, demonstrating that *JNM1* is not an essential gene for yeast growth under normal laboratory conditions. Low stringency Southern blot analysis of genomic DNA from a *jnm1-Δ1* haploid, JM127, digested with several restriction endonucleases, revealed no bands of hybridization (data not shown), indicating that *JNM1* is probably a single copy gene. CHEF gel electrophoresis, hybridization of a probe to an ordered set of phage λ clones containing yeast DNA, and tetrad analysis revealed that *JNM1* resides at a unique position on chromosome XIII, 9.0 cM from *SUP8* and 11.8 cM from *ADE4* (see Materials and Methods), confirming that *JNM1* is a novel gene.

jnm1-Δ2 and *jnm1-Δ3* mutants (Fig. 1 *C*) were constructed and found to have phenotypes identical to the *jnm1-Δ1* mutant as well as the original *jnm1-1* mutant. It is therefore possible that the original *jnm1-1* mutation acts as a null mutation. Most of the data presented in this paper utilized the *jnm1-Δ2* or *jnm1-Δ3* mutations. The *jnm-Δ1* mutation, a total deletion of the *JNM1* gene, was avoided because deleted sequences could potentially alter regulatory sequences upstream of the nearby open reading frame (Fig. 1 *A*), possibly creating a new phenotype which could not be solely attributed to a *jnm1* null mutation. However, we have not observed any phenotype difference between the *jnm1-Δ1*, *jnm1-Δ2*, and *jnm1-Δ3* alleles.

Sequence Analysis Predicts Jnm1p to Have Regions of Coiled Coils

The DNA sequence of the *JNM1* gene and flanking sequence is presented in Fig. 2. Conceptual translation of the *JNM1* open reading frame reveals a protein of 373 amino acids with an unmodified mol wt of 43,620 and an estimated pI of 4.65. No significant homology to other proteins was found in a search of Genbank data base sequences (version 76) using the FastA program. However, Jnm1p was found to have slight homology (less than 20% identity) to proteins which are known to have coiled coil structures, such as myosin. Like other coiled coil proteins, a large portion of Jnm1p is predicted to have α-helical secondary structure (Fig. 3). A coiled coil prediction computer program (Lupas et al., 1991) reveals three distinct regions of Jnm1p which show a strong probability of forming coiled coils. These putative coiled coil domains of Jnm1p have the typical heptad periodicity seen in other coiled coil proteins, with the first and fourth amino acids having a high proportion of hydrophobic amino acids (Fig. 3).

Jnm1 Mutants Are Sensitive to Temperature Extremes

Growth rates of a *jnm1-Δ2* strain, JM118, and a congenic wild-type strain, JC482, were determined at 11, 30, and

```
GGATCCAGGAAGCTTGGACGATGTGGGAACTATCAGTAGATCTAGGCCGTCTGGATTTCCCTTAGAATTAGTTAAAACATTTGGAAATCTGAAGATCCCG   100 bp
TCAAATTCATCGATCAAATTAACTCGTAGCTTTTCTGCCTTAATAAAATTGTTCTTAAATGCATCTGAACAAAGATTATAATTACCTAGAATGATTCTAT   200
TCTTAACTTCTGTTCCGAATTTGGACCTAGTAGGTGCGAATAAAATACCGTCTTTTATATCGAGTTCTGAATCTCTGTATCCATATCTGATACCATCATA   300
CCTTGATAAATTGGAAGCCGCTTCAGCGGGTGATAGCGTATAATAAATCGGTAAACAGTTTTTTACAGATGGAATGGATACAGGGTATATTTCAAGCCCT   400
AAATTTATCAGCTTTTCTAGTAAGGATAAATATAATCTGTGGAACCCAATGGGCATACTTTCATGGCTAAATTCCTTTACAATTCCTACCTTTAAAGGTC   500
TCCTAACCTTTTTATTCCCTTCTATCAATTCACGCAATTCCACACTTAAGGAAGTGGGATCTTTCATGTCATATTTATCGAGCGTATGAAATACTTTTCG   600
CAAGACGTTTATCTTTTTGCTAAGTATGCCAACAGTGTCTAAAGATTGAGAATACGCTATTACGCCAAATCTTGACAACCGTCCATAGGACGGCTTGAAT   700
CCTAAAACAGATCCATAGCATGCGGGGAGCCTAACGGAGCCACCAGTATCTGTTCCCAAGGCAAAATCGACTAGATCGCAAGCAACGCTTGCAGCGGCTC   800
CAGACGATGAACCTCCCATGATCTTCTTGTCCTCATGAGGATATAAAGGGTTAATTACGGGCCCTCTTATTGAATGTACTCCCCCAGAACCCATTCCAAA   900
TTCATCTAAATTTGTCTTGCCTAAGATATGCACTCCTGCCTGTTTTAATAGTTTCACTACTGTTGCATCGAAGGGAGACTTGAAATTCTCAAGTATATGT  1000
GAGGCACATGTGGTTGGAAAATCTTTTGTAACTATATTATCCTTGATACTGGCAACGCAACCTGTCAATGTTTCTTTTGTACCTTTTTTATTTGTGATTG  1100
AATAAGGAGATGGATTGATACTAGTGAAAATATTATATTTTGATTGAAAACTAGATAATCTTTCGATTGATTCTTTTAAGGAGCGTTTCAGTGGCATTTT  1200
TGTATAATCAAAGTTAGGACTCCAATTGAGGGGCCATCTTTCCAGCACAAATAATAGTGTTTACAAGTATAGATGTACTATTACTTTTTGGGAGCCAAT  1300
GCATTTCAAAAAAAAAAAGAAGAGCAGATAAGTCATGAGGCTAAGAAAGATAAAGAAATCTACTGGTTG ATG AAC GTC ATA GAT TTA AGT      1390
                                                                          M   N   V   I   D   L   S        7 aa

GAT CCT GCC ATC AAT GTG GAT TAT GAT AGC TTG ATT GGC ATT GAC AAT GAG GAA TCT CAA GAA ATT TTT GAA AAT   1465
 D   P   A   I   N   V   D   Y   D   S   L   I   G   I   D   N   E   E   S   Q   E   I   F   E   N    32

GAA GTG AAG GAA GAT GGA CAA CAA GAA GAG CAG GAA GAA GCA TCT TCA AGA AAA GAT GGG CTC ATC GTT GAA CCA   1540
 E   V   K   E   D   G   Q   Q   E   E   Q   E   E   A   S   S   R   K   D   G   L   I   V   E   P    57

GGG AGA GAT GTT GAG AGT TTG AGA AGG GCT ATT CGA GAT CAG TTG CTT TTC AAG ATA CAT AGA CAA AAC CAA TCA   1615
 G   R   D   V   E   S   L   R   R   A   I   R   D   Q   L   L   F   K   I   H   R   Q   N   Q   S    82

GAC TGT GCA GAT GCG AGA AAG TTG AGT AGC GAT GAA GAA GAT GAA AGT CGG CAA CAG AAA TTA GAA AGA ATA AGA   1690
 D   C   A   D   A   R   K   L   S   S   D   E   E   D   E   S   R   Q   Q   K   L   E   R   I   R   107

GAA GAA TTG GAG GAG TTG AGA ATA GAA AAT TTA ACA TCT GAA ATG CAA ACT GAA ATC AAG GAA TTG TGC GAA ATT   1765
 E   E   L   E   E   L   R   I   E   N   L   T   S   E   M   Q   T   E   I   K   E   L   C   E   I   132

CAA TCA AAA CTG GCG ACA GAA TCA TCT AGT AGA TTG ACA AAT TTG AGG AAG AAG CTT CTC GAA ACA TAT GAA GGC   1840
 Q   S   K   L   A   T   E   S   S   S   R   L   T   N   L   R   K   K   L   L   E   T   Y   E   G   157

CAA GAT ACC GTG ATA TTG CCA AAC ATA ATT CTT GAT ACG AGT AAT ATC AAA AGA TTG CAA AAG TTA GAT CAG AAA   1915
 Q   D   T   V   I   L   P   N   I   I   L   D   T   S   N   I   K   R   L   Q   K   L   D   Q   K   182

ATA TCC CTG ATG GAA CGT TTT GTT GGC ATA GCA GAA GCT TTG GAG GCA GAA GAA GAA AGG AAA TCG GTT CAT AGT   1990
 I   S   L   M   E   R   F   V   G   I   A   E   A   L   E   A   E   E   E   R   K   S   V   H   S   207

AAA GTC AAT GAA CTA TAT AGA AGT ATT CAA CTT TTA CAA GGC GAT GAT AAG GCG GAA GGA AAG CTG CAA AAG TTC   2065
 K   V   N   E   L   Y   R   S   I   Q   L   L   Q   G   D   D   K   A   E   G   K   L   Q   K   F   232

CGG GAT AGA CTC GTG GAA CTG AAC GAG GAA TTT GAA AAC TCA TTG TTA GGC AAG AAA ATA CAA CAG GAC TTG AGG   2140
 R   D   R   L   V   E   L   N   E   E   F   E   N   S   L   L   G   K   K   I   Q   Q   D   L   R   257

TTG AAA GAT GAC ACC GTG AAC AAG CTT GTT ATG CCC GAA AAC AAA GTA AAA GAG ATA AAT AGT ATG TAT TCC ATG   2215
 L   K   D   D   T   V   N   K   L   V   M   P   E   N   K   V   K   E   I   N   S   M   Y   S   M   282

TTC AAG CAA TAT CAA GAT TCA CTA CCA CTG CTG GCG GAG AGG ATG AAA AGT CTC AAT AAA ATG AAC AAC AGG GTG   2290
 F   K   Q   Y   Q   D   S   L   P   L   L   A   E   R   M   K   S   L   N   K   M   N   N   R   V   307

ATC GAG GTG TAC GAA ACC ACG AAA GGG CTG GAT TCA CAA ATA ACC AGC ATC CAA GAA CAA GGA AAA GTT TGG CTA   2365
 I   E   V   Y   E   T   T   K   G   L   D   S   Q   I   T   S   I   Q   E   Q   G   K   V   W   L   332

AAG GCT TTA AAT GAG CTG GAT AAA AAA TTC GAT GAA CAA GAG GTT AAA ATT CGC GAA AAT ATG GAG CAG ATC AGG   2440
 K   A   L   N   E   L   D   K   K   F   D   E   Q   E   V   K   I   R   E   N   M   E   Q   I   R   357

CGT AAA ATT GAT ACC CTC GAA GAC GAA GCT CTA CAG AGA AAT AGC AAA TAAAAGGCGGAGAAATAATTTTATAAACCAATTTAA   2524
 R   K   I   D   T   L   E   D   E   A   L   Q   R   N   S   K                                       373

TTTCATTCTTCATTTTTTCGTCTCCATATGACAAAAAAATTGAAAATATGTGTGTGTATGTATATATAATAATAGTAATAATAACAATATGAAATATGAA   2624
ATATCCAAAATAAGAGCGGAAAACAGAAATTATCATAAAAAAGAAAAAAATAAAGTCTCTAAAGGGTATCAAGCGCTTATTTCTTCTTCATTCTACCAAA   2724
CAATCCCTTCTTCTTCTTCTTTTGCTTTTCCTCAGTCTGTACGTGTTGTTGTGGCTGATACACTGCTTGTTCACCATACATTTGACTGGAAGCACCACCC   2824
ACTTGCTGTGGCATACCGTTCGCATCGTAAGTCACAGCAGCACCAAACACAGGGAAATCAGGTCTTACGCGGAACCCGTAAGTTGGAGTCTCCAACTGTT   2924
GGGCCCAGACCGGGTCTCCGGAGACAGCATACTCGAAACTTCTTATAGTGTCCAAAGGTCTTTCGTCTCTTGCCCTAGTTGGATTCGATATATCTGCCTG   3024
TGTGATGGGTTGACCGAAAACATCACACAGAACATGACCTTCTTCGTTGGAAAAATAAGATTGTCTGTTCATGTTGTCGTGGAAGGTATCAGCAGCTTGT   3124
TCAAAAGGTTGGGCTTCCTGCACAGCGTCTAGAATAGGATCC                                                            3166
```

Figure 2. Nucleotide sequence of *JNM1* and the predicted amino acid sequence of the encoded product. The underlined bases 5′ to the JNM1 ORF represent the initiation codon in the complementary sequence for the truncated ORF (see Fig. 1 *A*). These sequence data are available from EMBL/GenBank under accession number Z25750.

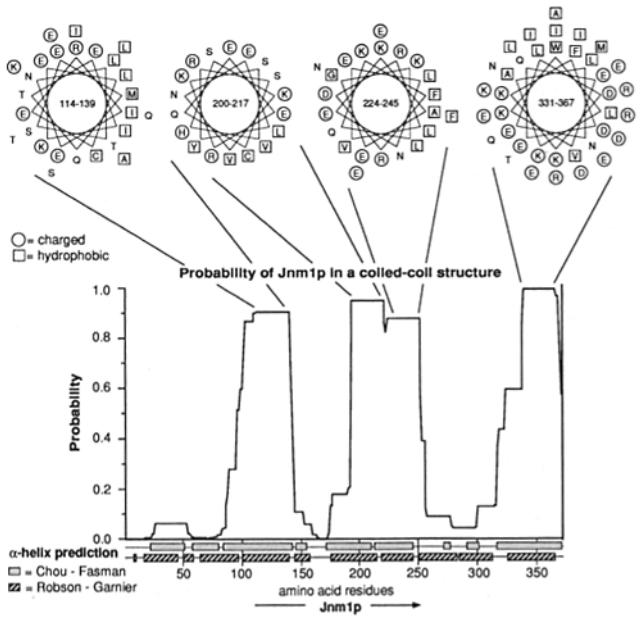

Figure 3. The probability that regions of Jnm1p adopt a coiled coil structure (ordinate) is plotted along the length of Jnm1p (abscissa) using the program of Lupas et al. (1991). The probability that JNM1p adopts α-helices is also plotted on the abscissa, using the Chou-Fasman and Robson-Garnier predictions from the MacVector program (IBI Inc., New Haven, CT) to calculate these probabilities. Sequences of Jnm1p predicted to adopt a coiled coil structure are plotted in helical wheel diagrams in which the protein sequences are in α-helices. □ and ○ denote hydrophobic and charged residues, respectively.

37°C. *jnm1-Δ2* and *JNM1* had nearly identical doubling times in YPD media at 30°C (96 and 90 min, respectively), but *jnm1-Δ2* had a longer doubling time at both elevated and reduced temperatures. At 37°C the doubling time of the *jnm1-Δ2* strain increased 35% over that of the *JNM1* strain (234 versus 173 min, respectively). At 11°C the doubling time of the *jnm1-Δ2* strain increased 147% over that of the *JNM1* strain (33.9 h for *jnm1-Δ2* versus 13.7 h for *JNM1*). The slow growth of *jnm1-Δ2* at 11°C is stable; we have not ob-

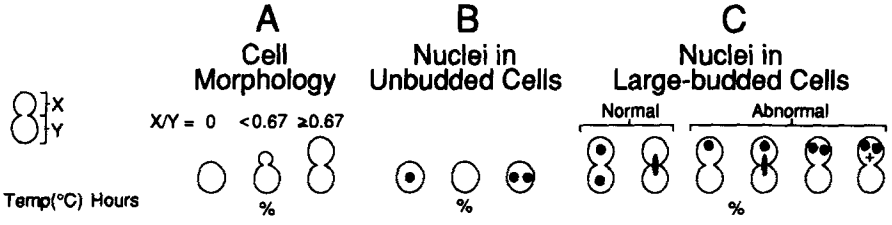

Genotype	Temp(°C)	Hours	A: X/Y = 0 (%)	A: <0.67 (%)	A: ≥0.67 (%)	B: 0 (%)	B: 1 (%)	B: 2 (%)	C: Normal		C: Abnormal (%)			
JNM1	36	6	51	19	31	100	0	0	81	13	3	3	1	0
jnm1-Δ2	36	6	47	25	28	100	1	0	58	14	21	2	5	0
JNM1	30		49	29	22	100	0	0	85	13	1	1	1	0
jnm1-Δ2	30		41	29	31	100	1	0	67	20	3	2	10	0
JNM1	13	22	33	38	29	100	0	0	82	13	4	1	1	0
jnm1-Δ2	13	22	28	37	35	99	0	1	47	8	23	3	20	0
JNM1	11	25	42	31	27	100	0	0	83	11	4	1	2	1
jnm1-Δ2	11	25	29	24	47	99	1	0	26	10	17	2	50	2
JNM1	11	50	41	30	29	100	0	0	78	7	10	2	5	0
jnm1-Δ2	11	50	20	19	60	99	2	0	4	2	25	1	68	1

Figure 4. Cell morphology and nuclear distribution in *jnm1-Δ2* and *JNM1* cells grown in liquid medium. *jnm1-Δ2* (Strain JM120) and *JNM1* (strain JM123) were grown in YPD at 30°C to log phase and aliquots were shifted to 11, 13, or 36°C. At the designated times, cells were harvested, fixed, and stained with DAPI to visualize nuclei. Data is presented in percentages. Numbers were rounded to the nearest integer, therefore row totals may not equal 100. (*A*) Cell morphology with respect to bud size and presence. n = 133–196 for each culture. Using chi square analysis a significant shift in the distributions of cell morphologies is detected at 11°C after 25 h ($p < 0.0025$) and at 11°C after 50 h ($p < 0.0005$). (*B*) The nuclear distribution in unbudded cells was determined and depicted as the percentage of total unbudded cells. n = 200 for each culture. (*C*) The nuclear distribution in large budded cells was determined and depicted as the percentage of total large budded cells. n = 200 for each culture.

served any spontaneous revertants that have acquired a more rapid growth rate. To more precisely determine the temperatures to which *jnm1-Δ2* was sensitive, tetrads from a heterozygous *jnm1-Δ2/JNM1* diploid (strain JM132) were dissected on YPD medium and the plates immediately incubated at 38, 36, 34, 30, 24, 16, 13, or 11°C allowing for germination and colony growth at that respective temperature. A noticeable growth defect of the Ura$^+$ colonies (*jnm1-Δ2*) could be detected at 38, 36, 16, 13, and 11°C but no growth defect could be detected at 34, 30, or 24°C.

jnm1 Mutants Display Abnormal Nuclear Migration Phenotypes and Accumulate as Large Budded Cells When Grown at Low Temperatures

To determine if the growth defect of *jnm1-Δ2* at either the elevated or reduced temperatures was accompanied by a cell cycle-specific defect, we grew *jnm1-Δ2* and *JNM1* strains to log phase at the permissive temperature of 30°C and then shifted aliquots to 11, 13, or 36°C. After a defined period the cells were fixed with ethanol and stained with DAPI to visualize cell morphology and the nuclear regions. These results are presented in Fig. 4 *A*. At 30 and 13°C, *jnm1* cells may have a slightly higher frequency of large budded cells than the wild type. However, at 11°C after 50 h of growth, 60% of the cells had large buds, many of these with very large buds creating a dumbbell shape. Although *jnm1* cells also had a slight growth defect at elevated temperature, we observed no obvious cell cycle defect at this temperature.

The dumbbell morphology is often associated with mutations that block the cell cycle prior to cytokinesis (Pringle and Hartwell, 1981). To better characterize the mutant phenotype of *jnm1* we stained cells with DAPI to visualize nuclei. In wild-type strains, large budded cells are indicative of cells in G2 or M phase. Their nuclei are normally located in the bud neck, or in the case of cells that have completed mitosis, the divided nuclei are found in both the mother and the bud. As shown in Fig. 4 *C*, greater than 97% of large budded wild-type cells that have been grown at 30°C have nuclei in one of these two normal configurations. However, only 87% of nuclei of large budded cells from the *jnm1* mutant were normal and a majority of the abnormal cells contained two nuclear staining bodies in one cell lobe. The percentage of cells with the normal morphology dramatically decreased with decreasing temperature and increasing time. After one doubling at 11°C (50 h) only 6% of large budded cells from the *jnm1* strain had a normal nuclear morphology and a majority of the abnormal cells either contained one nucleus or contained two nuclei in one cell body. Unbudded *jnm1* cells appeared normal with respect to the number of nuclei. As shown in Fig. 4 *B*, no significant increase in unbudded cells with multiple nuclear staining or anuclear cells was observed in *jnm1-Δ2*.

In the large budded *jnm1* cells the two cell bodies were often equal in size and it was not possible to distinguish between the mother cell and the growing bud. We could therefore not determine if the two nuclear staining regions were always present in the mother cell, the bud, or randomly associated with both. To distinguish between these possibilities we stained *jnm1-Δ2* cells that had been grown for 50 h at 11°C with DAPI and Calcofluor, a chitin-specific stain that allows visualization of bud scars. Mother cells have at least one scar while buds have none. Nuclei were associated with the cell lobe that contained visible bud scars in every large budded cell that contained multiple nuclei (n = 100). We conclude that the major defect we observe in *jnm1* at low temperature is a failure to distribute one set of chromosomes to the daughter cell during mitosis. We did observe that a significant proportion of the large budded *jnm1* cells contained only a single mislocalized nucleus. This could reflect a separate phenotype but it is possible that at least a proportion of these cells have two nuclei, one directly on top of the other.

jnm1 mutants also showed a reduced growth rate at high temperature but we did not observe any change in the percentage of large budded cells at higher temperature (Fig. 4

Figure 5. Sporulated culture of strain JM153, a *jnm1/jnm1* homozygous diploid showing two asci with eight spores and an attached bud. Six spores are visible in the ascus at the lower right while only four of eight spores are visible in the ascus on the far left. Bar, 5 μm.

A). We did, however, observe a significant increase in cells with a single nucleus among the large budded cells and a smaller number of cells with two nuclei in one cell body. It is therefore possible that the reduced growth rate of *jnm1* at high temperature is due to a different defect than that observed at low temperature.

Another observation that points to a defect in nuclear migration in *jnm1* mutants is that a high proportion of asci from sporulating cultures of homozygous *jnm1/jnm1* diploids contain more than the normal four spores per ascus. The photomicrograph in Fig. 5 of a sporulated *jnm1/jnm1* diploid reveals asci with 8 spores and a bud attached to each ascus sac. Approximately 15% of the asci from *jnm1/jnm1* diploids sporulated at 30°C were observed to have this structure. Eight-spored asci were very rarely seen in a heterozygous *jnm1/JNM1* diploid and never observed in homozygous *JNM1/JNM1* diploids. This unusual phenotype has been observed for *num1* mutants (Kormanec et al., 1991), which have been reported to have a defect in nuclear migration. If a nucleus does not properly migrate between the mother cell and bud, upon mitosis the mother cell will contain two nuclei and the bud will remain anucleate. Initiation of meiosis could result in a mother cell that contains eight spores. We have dissected these eight-spored asci and find that a majority of the spores are viable (data not shown).

jnm1 Mutants Have Misoriented Spindles and at Low Temperature Have Elongated Astral Microtubules in Large Budded Cells

Both nuclear migration and spindle orientation have been shown to be dependent on the presence of astral microtubules. To determine if the *jnm1* mutation influences astral microtubule structure or spindle orientation, we viewed microtubules by indirect immunofluorescence using an anti-α tubulin primary antibody and a FITC-labeled secondary antibody. Mitotic spindles in wild-type cells align along the mother/bud axis during mitosis. When *jnm1* mutant cells are grown at 30°C, the spindle structure in large budded cells displaying a binucleated phenotype is seen to connect the

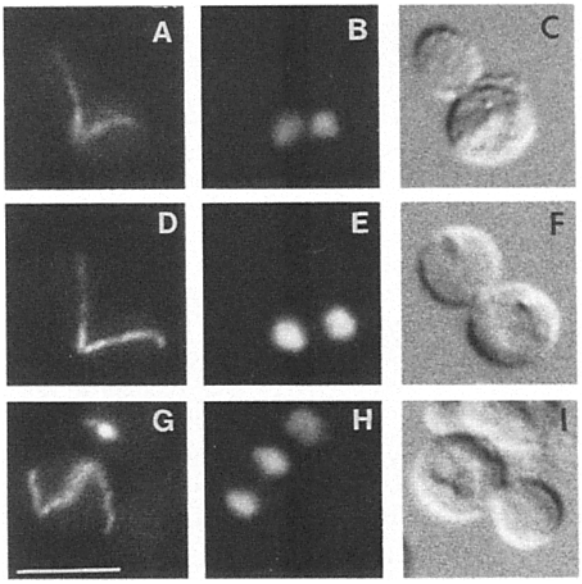

Figure 6. Micrographs of *jnm1* cells that contain two abnormal DAPI staining regions. *jnm1-Δ2* strain JM122 was grown to log phase in YPD at 30°C. Cells were harvested, fixed, and prepared for microscopy as described in Materials and Methods. The cell present in each row is representative of those large budded cells that have mislocalized nuclei. Microtubules were visualized by indirect immunofluorescence in *A*, *D*, and *G* using the anti-α tubulin antibody YOL1/34 and a FITC-labeled goat anti-rat IgG secondary antibody. Nuclear regions were visualized with DAPI in *B*, *E*, and *H*. Nomarski images are presented in *C*, *F*, and *I*. Bar, 5 μM.

Figure 7. Micrographs of wild-type (JM120) and *jnm1-Δ2* (JM123) cells grown in YPD at 11°C for 50 h. Wild-type (*A*, *B*, and *C*) and *jnm1* cells (*D*, *E*, and *F*) were harvested, fixed, and prepared for microscopy as described in Materials and Methods. Microtubules were visualized by indirect immunofluorescence, as in Fig. 6, in *A* and *D*. Nuclear regions were visualized with DAPI in *B* and *E*. Nomarski images are presented in *C* and *F*. Bar, 5 μm.

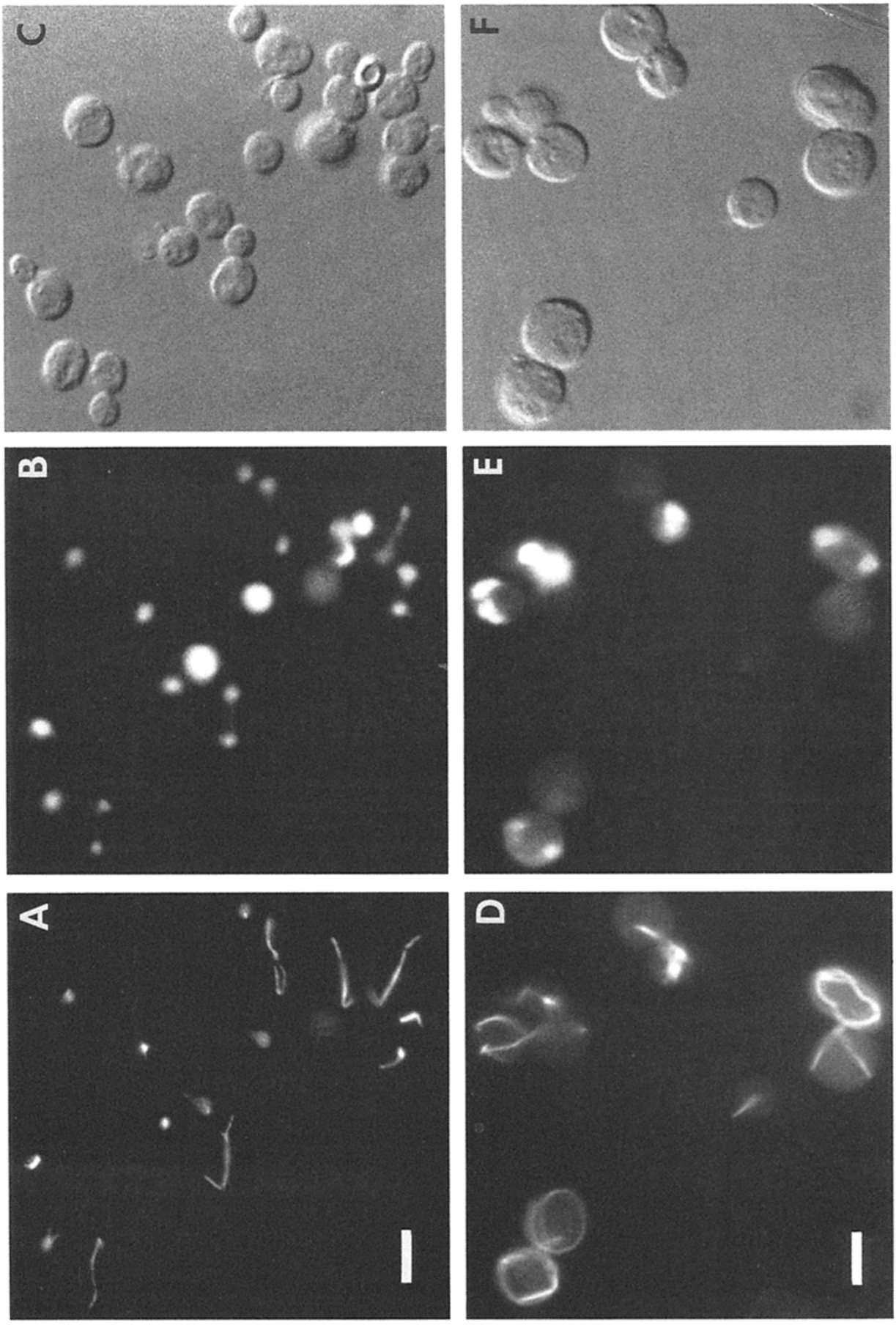

two DAPI staining regions, but is often misaligned with respect to the mother/bud axis. That a spindle connects the two DAPI staining regions indicates nuclear division has not been completed in these cells. For a more complete analysis, 21 randomly chosen large budded cells displaying a binucleated phenotype, as determined by DAPI staining, were photographed. Three representative cells are displayed in Fig. 6. 20 of the 21 cells contained a single spindle connecting each DAPI staining region indicating an undivided nucleus in late mitosis. The one exception appeared to have two SPBs, one associated with each DAPI staining region, but lacked a spindle. In this cell a microtubule bundle emanated from only one of the two SPBs but it could not be determined whether these microtubules were intranuclear or cytoplasmic. 14 of the 20 cells in late telophase had a straight spindle connecting the two SPBs while the remaining 6 cells contained a bent spindle, sometimes bending around the outside of the cell forming a horseshoe pattern. In most of the cases the spindles were not aligned along the mother/bud axis, as is normally the case in wild-type cells. If an imaginary straight line is drawn between the two SPBs and extended toward the mother/bud neck, only in two of the 21 cells would the line enter the bud through the bud neck.

Astral microtubules were visible in 20 of the 21 cells with the single exception described above. Although the SPBs in most of these cells were misoriented with respect to the mother/bud axis, in all cells with astral microtubules, an astral microtubule bundle extended to the mother/bud neck and the microtubule bundle entered the bud in 17 of the 20 cells. It appears that although the nucleus is not in the proper position within the cell, the astral microtubules are able to recognize and in most cases enter the bud. The SPB closest to the mother/bud neck gave rise to the astral microtubules which reached to the mother/bud neck in 17 cells. In two cells it could not be determined from which SPB this astral microtubule arose, and in one cell the two SPBs were approximately the same distance from the neck. In this respect there is at least some orientation of the SPBs with respect to the mother/bud neck.

Aberrant microtubules are most obvious when *jnm1* cells are grown at temperatures below 13°C. In Fig. 7, wild-type and congenic *jnm1* strains were grown for 50 h at 11°C, fixed, and stained with DAPI and an anti-tubulin antibody. The wild-type cells are in different stages of the cell cycle and normal mitotic spindles are visible in cells in mitosis (Fig. 7 *A*). In contrast, the *jnm1* mutants accumulate as large budded cells with extremely long microtubules (Fig. 7 *D*). Unbudded cells or cells with small buds do not have this phenotype; thus, the elongated astral microtubules appear to be specific for the large-budded stage of the cell cycle.

The spindle structure in cells with elongated astral microtubules is not clear. Often a microtubule bundle is seen to connect the two DAPI-staining regions, however, this bundle does not run along the axis between the two DAPI-staining regions in a binucleated cell, but is often bent and appears to be pushed along the periphery of the cell (Fig. 7 *D*). In many cells the winding of the astral microtubules around the mother cell and bud is so severe that it is not possible to tell from which SPB a particular astral microtubule bundle arises. At 13°C most of the large budded, binucleated cells have an elongated astral microtubule structure, but the winding is typically not as severe as at 11°C. The occasional binucleated cells in the wild-type background are never observed to have elongated astral microtubules, even at 11°C, nor are elongated astral microtubules observed in the wild-type or *jnm1* mutant cells grown at 36°C.

The observation that only large budded cells have the long astral microtubules suggests that the development of these structures is cell cycle dependent. To extend this observation we synchronized wild-type and *jnm1* cells in the G1 stage of the cell cycle with α factor at 30°C. One aliquot from each culture was shifted directly to 11°C while another aliquot was washed to remove the α factor prior to shifting to 11°C. Wild-type and *jnm1* cells were observed to enter the cell cycle with similar kinetics but the elongated astral microtubules were only observed in *jnm1* cells after these cells obtained large buds. *jnm1* cells held in G1 by the continued presence of α factor never developed the long microtubules observed in the logarithmically growing *jnm1* cells (data not shown).

jnm1 Mutants Are Only Mildly Sensitive to Antimicrotubule Drugs

Mutations which affect microtubule stability or structure have often been found to confer greater sensitivity or resistance to antimicrotubule drugs such as the benzimidazoles, benomyl and TBZ. To determine the sensitivity of *jnm1* mutants to benomyl and TBZ we placed saturated cultures of *jnm1-Δ2* and *JNM1* cells on plates containing different concentrations of benomyl or TBZ. The plates were incubated at 13, 24, or 37°C and scored when the cultures growing on plates without the drugs had become confluent. We observed the *jnm1* strain was only slightly more sensitive to benomyl and TBZ than our wild-type strain at 24°C. For example, our wild-type strain was able to grow on plates containing less than 25 μg/ml benomyl but the *jnm1* strain was able to grow on plates containing less than 20 μg/ml benomyl (Table II). Although temperature influences the sensitivity of yeast cells to benomyl and TBZ, the *jnm1* strain was always only slightly more sensitive than the wild type. At 37°C, the *jnm1* mutant appeared to be slightly more sensitive to benomyl and TBZ when compared with the relative sensitivities at 13 and 24°C. However, the *jnm1* strain was also more sensitive to ethidium bromide and cycloheximide at 37°C relative to the wild-type strain, whereas at 24°C the *jnm1* strain and wild-type strain displayed the same sensitivities to these drugs. This may indicate that the *jnm1* cells are more permeable at higher temperatures and therefore more sensitive to

Table II. Sensitivity of jnm1 to Benomyl and TBZ

Drug	Temp °C	Drug concentration at which no growth is observed μg/ml		Measured increments μg/ml*
		JNM1	*jnm1-Δ2*	
Benomyl	37	60	40	5
Benomyl	24	25	20	5
Benomyl	13	8	7	1
TBZ	37	120	80	10
TBZ	24	110	80	10
TBZ	13	20	14	2

* Strains were dropped on media containing incrementally increasing amounts of drug starting at a concentration of 0.

benomyl and TBZ. The mild sensitivity to benomyl observed in the *jnm1* mutant is very distinct from that of the hypersensitive *tub* mutants (Schatz et al., 1986, 1988; Huffaker et al., 1988), or *cin* mutants (Stearns et al., 1990) which are often several times more sensitive to benomyl than the wild-type strain.

jnm1 Does Not Effect Karyogamy Efficiency or Chromosome Loss During Mitosis

If the absence of Jnm1p affects microtubule structures, other microtubule-dependent processes, such as karyogamy or chromosome segregation, might also be affected. We therefore assayed the efficiency of karyogamy and chromosome segregation in wild-type and congenic *jnm1* strains. Karyogamy efficiency is commonly measured by determining the ratio of cytoductants to diploid zygotes. Cytoductants are haploid cells that form prior to, or in the absence of, nuclear fusion after the cytoplasmic fusion of two mating cells. A cytoductant contains only one of the two haploid nuclei but it contains a mixture of cytoplasm from each of the two mating cells. By using both a cytoplasmic and a nuclear marker, cytoductants can be positively selected (see Materials and Methods). An increase in the ratio of cytoductants to diploid cells upon mating would indicate a defect in karyogamy. As shown in Table III, there is little difference in the cytoductant/diploid ratio for the mating of two wild-type strains and two *jnm1-Δ2* strains at 37, 30, or 13°C, implying there is no defect of the *jnm1* strains in karyogamy.

Chromosome loss was measured using a mating assay (Table IV). The mating assay quantifies the ability of a *MATa/MATα* diploid to mate with a haploid cell. *MATa/MATα* diploids are sterile but will regain the ability to mate if they become homozygous or hemizygous for chromosome III, on which the *MAT* locus is located. A diploid cell may become hemizygous for *MAT* by losing one copy of chromosome III or homozygous for *MAT* by a recombination event. Previous work has demonstrated that the predominant event leading to the loss of one of the two *MAT* loci in wild-type cells is due to chromosome loss (Gerring et al., 1990). However, any increase in mating efficiency of a *MATa/MATα* diploid could be due to an increase in chromosome loss, recombination, or both. As shown in Table IV, mating efficiencies for wild-type or homozygous *jnm1/jnm1* diploids were nearly identical at 13, 30, or 36°C. The chromosome loss mating assay was corroborated by a red/white colony sectoring assay measuring the loss of a yeast artificial chromosome using a similar system to Hieter et al. (1985). At 13°C, there was no significant difference in the rate of loss of this yeast artificial chromosome in a *jnm1-Δ3* strain versus the wild-type (data not shown). Together, the normal rates of karyogamy and chromosome loss in *jnm1* mutants suggest that *JNM1* does not have a general role in microtubule metabolism but is specifically required for nuclear migration during mitosis.

Table III. Cytoductant to Diploid Ratio at Various Temperatures

Strains	Genotype	Temp °C	C/D* ratio	Mating efficiency
KT113 × JM150	*JNM1* × *JNM1*	37	0.014	57%
JM126 × JM151	*jnm1-Δ2* × *jnm1-Δ2*	37	0.018	30%
KT113 × JM150	*JNM1* × *JNM1*	30	0.0011	66%
JM126 × JM151	*jnm1-Δ2* × *jnm1-Δ2*	30	0.0025	44%
KT113 × JM150	*JNM1* × *JNM1*	13	0.011	48%
JM126 × JM151	*jnm1-Δ2* × *jnm1-Δ2*	13	0.012	40%

* C/D = cytoductant/diploid ratio.

Table IV. Mating Efficiency of MATa/MATα Diploids Measured by Fluctuation Analysis

Strain	Relative Genotype	Temp C°	Production of mating efficient cells/cell division
JM152	*JNM1/JNM1*	36	1.18×10^{-6}
JM153	*jnm1-Δ2/jnm1-Δ2*	36	8.41×10^{-7}
JM152	*JNM1/JNM1*	30	2.62×10^{-6}
JM153	*jnm1-Δ2/jnm1-Δ2*	30	2.06×10^{-6}
JM152	*JNM1/JNM1*	13	1.48×10^{-5}
JM153	*jnm1-Δ2/jnm1-Δ2*	13	1.41×10^{-5}

A Jnm1p:β-galactosidase Fusion Protein Localizes Predominately to a SPB

Our preliminary approach to localize Jnm1p has been to construct a Jnm1p:β-galactosidase fusion protein that retains biological activity and determine the location of this protein by indirect immunofluorescence. The entire coding sequence of the *JNM1* gene was fused to the *lacZ* gene of *E. coli* as described in Materials and Methods. Plasmid pJM1470 containing the *JNM1:lacZ* fusion and *URA3* was transformed into a *jnm1-Δ1* strain (JM140) such that the entire plasmid recombined at the *jnm1-Δ1* locus. The structure of the integrated plasmid is diagrammed in Fig. 8 *A*. This gene fusion, which is transcribed from the endogenous *JNM1* promoter and is present at only a single copy on chromosome XIII, is able to fully rescue the cold-sensitive growth phenotype (Fig. 8 *B*) and suppress the abnormal astral microtubule phenotype (data not shown) of *jnm1*.

Yeast strains that contain the integrated *JNM1:lacZ* fusion were stained with anti-β-galactosidase and anti-tubulin antibodies to visualize both the Jnm1p:β-galactosidase protein and microtubules. The anti-β-galactosidase antibody stained all the *JNM1:lacZ* cells with a nonuniform background fluorescence and some of the cells with a single, small, intensely fluorescent spot. Visualization of this spot was sensitive to long fixation times in formaldehyde and we found that fixing cells for 30 min on ice in 3.7% formaldehyde gave consistent results for the visualization of the fluorescent spots. Unfortunately, under these fixation conditions we also found that microtubule structures were less efficiently preserved than with longer fixation times and at higher temperatures. Nevertheless, we were able to simultaneously observe both microtubules and β-galactosidase staining. We determined the location of the spot relative to the SPB, microtubules, and bud in 211 JM142 cells chosen at random. This data is summarized in Fig. 10. We also visualized the β-galactosidase and microtubule pattern in a diploid strain that expressed the Jnm1p:β-galactosidase fusion protein and found the same overall pattern of expression. Because diploid cells are larger than haploids we have presented representative fields for a diploid strain in Fig. 9. Our findings are summarized as follows. First, all cells expressing Jnm1p:βgalactosidase

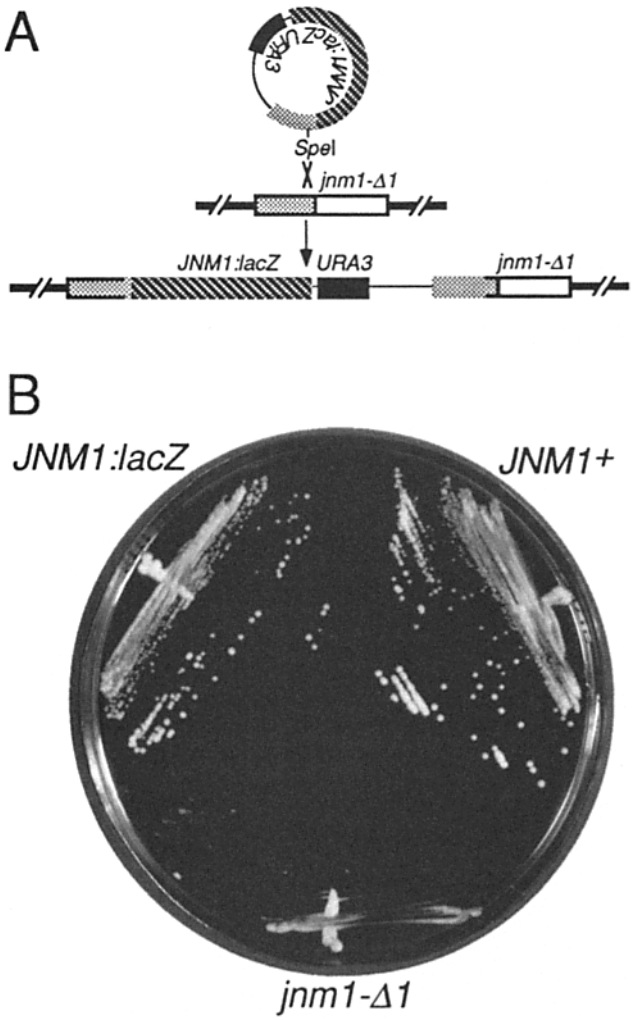

Figure 8. Construction of a *JNM1:lacZ* fusion gene and its biological activity. (*A*) Plasmid pJM1470, which contains the *JNM1:lacZ* gene fusion and *URA3*, is depicted as a circle. This plasmid was integrated into the yeast chromosome at the *jnm1-Δ1* locus by transforming strain JM140 with plasmid pJM1470 cut with the restriction enzyme SpeI. The gray stippled box represents DNA sequence upstream of the *JNM1* ORF found both on the plasmid and on the chromosome. Boxes with a black border represent DNA originating from chromosomal DNA while boxes with no border are of plasmid origin. Thick lines represent chromosomal DNA and thin lines represent plasmid DNA. (*B*) Photograph of wild-type (JM121), *jnm1-Δ1* (JM140), and *JNM1:lacZ jnm1-Δ1* (JM142) strains which were plated on YPD and incubated for 3 wk at 11°C.

stained with a nonuniform punctate pattern (Fig. 9, *A* and *D*) that was not observed in the control (Fig. 9 *G*). Second, in addition to this background pattern of staining about 35% of the cells contained a single intensely staining spot. Only a single spot per cell was observed in either haploid or diploid cells ($n > 1{,}000$). The spot is most often associated with the SPB; 80% of the spots in cells with an unduplicated or unseparated SPB were at or near the SPB (Fig. 10). The colocalization of anti-β-galactosidase (Fig. 9, *A* and *D*) and anti-microtubule staining (Fig. 9, *B* and *E*) can be seen in many of the cells. The association was less strong in cells at later stages of the cell cycle. In cells with short spindles, indicative of cells in G2 or early M phase, only 73% of the spots were at the SPB and in cells with an extended spindle, only 34% of the spots were at the SPB.

A third key observation is that the spot was most often associated with the bud. In cells with short spindles the spot was either in the bud or at the SPB nearest the bud. A clear example of this localization pattern is shown in Fig. 9, *A* and *B* where a spot is clearly near the end of the spindle closest to the bud. This polarized pattern was more obvious in cells with elongated spindles. 19 of 23 spots found in cells with elongated spindles were in the bud.

Where is the spot located in the significant minority of cells in which it is not associated with a SPB? Clear association with another organelle or structure is not usually observed in those cells that contain either a single SPB or short spindle but these spots are often found at the cell periphery. A clear example of this location is presented in Fig. 9 *D* (*small arrow*). However, in cells with an elongated spindle, the spot is often associated with the astral microtubules. An example of this pattern can be found in Fig. 9 *D* (*large arrow*) where the spot overlaps the astral microtubule staining in Fig. 9 *E*. Spots not localized to the SPB or astral microtubules, such as the one identified by the small arrow in Fig. 9 *D*, might also be associated with an astral microtubule, but our inability to carefully preserve astral microtubules prevents us from making a more definite conclusion about the location of the Jnmlp:β-galactosidase fusion.

Discussion

The Spindle Migration Defect in jnm1 Causes a Block in Late Mitosis and Cytokinesis

The predominant defect we observe in *jnm1* mutants is cells with two nuclear staining regions in the mother cell. At 30°C, most of these binucleate cells have a single anaphase spindle indicating a nucleus in late mitosis. The frequency of cells with this phenotype increases with decreasing temperature. The spindle migration defect in *jnm1* mutants does not result in cell death: even at 11°C, where over 55% of cells have large buds and two DAPI staining regions, we seldom observe anuclear cells, or cells with more than two nuclear staining regions. At this temperature, *jnm1* mutants continue to grow exponentially, indicating that the vast majority of cells are eventually able to complete the cell cycle successfully. The nuclear migration defect observed in *jnm1* mutants suggests to us a model in which Jnmlp has a primary role

Figure 9. Indirect immunofluorescence micrographs of a *JNM1:lacZ* fusion and a *JNM1* strain stained with anti-β-galactosidase and anti-β tubulin antibodies. *JNM1:lacZ* strain, JM181, (*A–F*) and wild-type strain, JM183, (*G–I*) were grown at 30°C in YPD, harvested during exponential growth, fixed, and prepared for immunofluorescence as described in Materials and Methods. (*A*, *D*, and *G*) Cells stained with a rabbit anti-β-galactosidase polyclonal antibody. (*B*, *E*, and *H*) Cells stained with the anti-β tubulin antibody 4A1. (*C*, *F*, and *I*) Cells stained with DAPI. Bar, 5 μm.

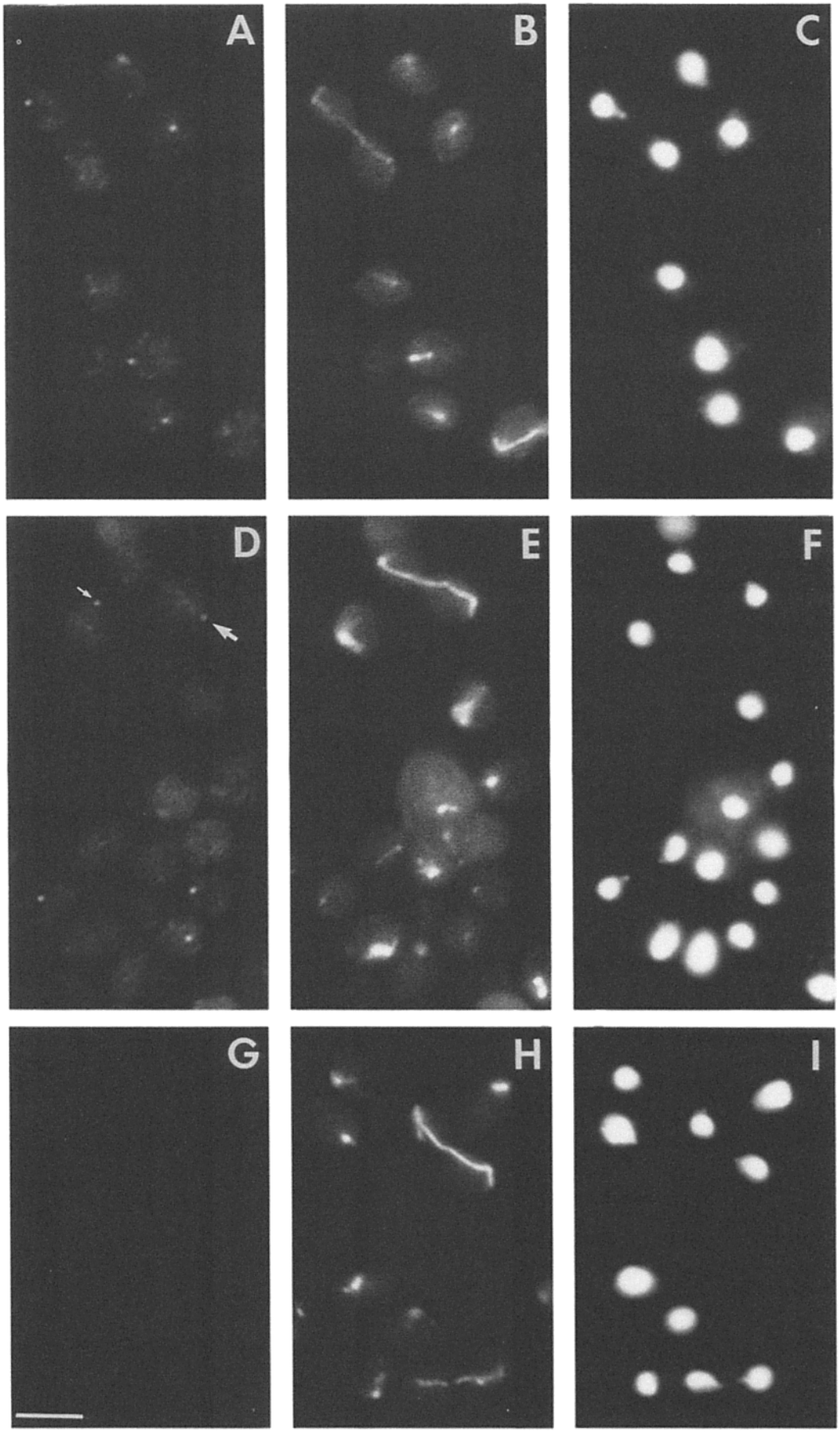

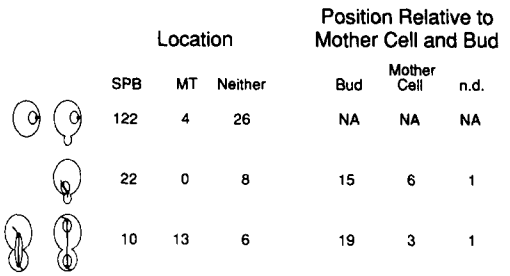

	Location			Position Relative to Mother Cell and Bud		
	SPB	MT	Neither	Bud	Mother Cell	n.d.
	122	4	26	NA	NA	NA
	22	0	8	15	6	1
	10	13	6	19	3	1

Figure 10. Localization of the anti-β-galactosidase staining spot in *JNM1:lacZ* cells (strain JM142) at different stages of the cell cycle. The localization and position of the spot was determined as described in Materials and Methods. The small, filled-in circles represent the SPBs, the open circles or ovals represent DAPI staining regions, and the straight black lines emanating from the SPBs represent microtubule structures. The top row contains fluorescent spot localization data in unbudded or small budded cells with either unduplicated or unseparated SPBs. The middle row contains localization data for cells containing nuclei with separated SPBs and a short spindle structure. The bottom row contains localization data for cells during late mitosis with an elongated spindle. The first three columns contain localization data of the fluorescent spot with respect to the SPB and astral microtubule structures. Of the spots localizing to the SPB or astral microtubules, the position of the spot was determined relative to the mother cell and bud (last three columns). In cells with pre-anaphase spindles, a fluorescent spot at the SPB closest to the bud was considered to be positioned towards the bud and therefore classified as a bud position. The position of the fluorescent spot could not be determined relative to the mother cell and bud in one cell with a pre-anaphase spindle because the two SPBs were equidistant from the neck, and in one large budded cell in late mitosis because the mother cell and bud were of a similar size.

in nuclear migration and/or spindle orientation. We favor the hypothesis that the misalignment of the spindle is responsible for the anaphase delay although we cannot rigorously exclude the possibility that Jnm1p also has a direct role in anaphase. However, in support of our hypothesis, we do not observe an accumulation of cells arrested with an anaphase spindle properly aligned at the bud neck, implying that the anaphase delay is an indirect consequence of the nuclear migration defect.

If the anaphase delay in *jnm1* mutants is an indirect consequence of the nuclear migration defect, a checkpoint or blocking mechanism operates to prevent cells with a misaligned spindle from completing mitosis. If such a blocking mechanism does exist it is interesting that it does not appear to function in some other mutants with a nuclear migration defect. The *tub2-401* mutant, which is also defective in nuclear migration at a semi-permissive temperature (18°C) continues rounds of nuclear division in the complete absence of nuclear migration (Sullivan and Huffaker, 1992). *bik1* mutants exhibit defects in spindle migration and give rise to multinuclear and anuclear cells (Berlin et al., 1990). In contrast to *jnm1* mutants, which have well developed astral fibers, *tub2-401* and *bik1* mutants have defects in astral fiber formation. Is it possible that the mechanism that prevents the completion of mitosis in binucleate *jnm1* cells requires astral fibers? The blocking mechanism that prevents the completion of mitosis in *jnm1* cells is likely to be distinct from that which prevents cytokinesis and mitosis in cells treated with anti-microtubule drugs and defined by the *bub* (Hoyt et al., 1991) or *mad* (Li and Murray, 1991) mutants. Loss of microtubules results in G2 arrest whereas the *jnm1* cells accumulate in late mitosis.

Jnm1p May Have Multiple Roles in Cell Division

jnm1 deletion strains exhibit two abnormal nuclear staining patterns in large budded cells. Cells are found with the aforementioned binuclear phenotype but cells are also observed with a single pre-anaphase nucleus that has not migrated to the bud neck. At 36°C, 21% of large budded cells have a single mislocalized pre-anaphase nucleus but only 5% of large budded cells have a binuclear phenotype. The frequency of mislocalized single nuclei drops to 3% at 30°C while the frequency of binucleate cells increases to 10% and continues to increase with reduced incubation temperature. The fact that these two abnormal phenotypes have different temperature profiles suggests that they may reflect separate events, both of which require Jnm1p, and are not simply different steps of the same process. An additional line of evidence that *JNM1* may have several independent functions is our observation that *SRK/SSD1*-containing plasmids suppress the weak temperature sensitive defect of *jnm1* (Wilson et al., 1991) but not the cold sensitive growth defect (data not shown).

jnm1 Mutants Accumulate Long Astral Fibers at Low Temperature

One of the most unique traits associated with *jnm1* mutants is the extremely long astral fibers that accumulate at low temperature. This trait could be a direct consequence of the *jnm1* mutation if, for example, Jnm1p were to have a role in anchoring astral microtubules to an attachment site in the bud (see below). Alternatively, the elongated astral microtubules may be a simple consequence of the mitotic delay. Perhaps astral fiber length is dependent on the length of time a cell spends at the *jnm1*-induced block in late mitosis. Whatever the reason for the long fibers, it is clear that Jnm1p is not simply a regulator of astral fiber length. Both wild type and *jnm1* mutants have microtubules of the same length at 11°C when maintained in G1 by the continued presence of α factor.

A Jnm1p:β-galactosidase Fusion Protein Has a Restricted Distribution

All cells that contain a single copy of a *JNM1–lacZ* gene fusion exhibit an irregular, punctate pattern of staining with anti-β-galactosidase antibodies. However, ~35% of these cells also contain a single highly fluorescent region. Although our localization studies are preliminary, several conclusions can be made. First, only a single staining region is observed per cell. We have never observed two or more dots in a cell ($n > 1{,}000$). In this regard the Jnm1p:β-galactosidase protein most closely resembles a Kar1–β-galactosidase fusion protein that localizes asymmetrically to the single SPB nearest the bud (Vallen et al., 1992). The localization of the Jnm1p:β-galactosidase fusion is clearly different in that it is not always associated with a SPB. The second conclusion is that the staining region is often but not exclusively associated with the SPB. In cells with an unduplicated SPB or short spindle the spot is most often associated with a SPB, but is

less often associated with the same organelle in cells with long spindles. Finally, the staining region is usually in the bud or adjacent to it. In cells with short spindles the spot is near the SPB nearest to the bud while in cells with long spindles it is most often in the bud, irrespective of its association with the SPB.

We cannot rule out the possibility that the restricted localization of the Jnmlp:β-galactosidase hybrid is an artifact. However, several observations lead us to believe that the signal may reveal the actual location of Jnmlp. First, the hybrid is expressed from a single gene in the chromosome driven from the native *JNM1* promoter. The hybrid protein should therefore not be greatly overexpressed relative to the normal protein, excluding differences to protein stability. Second, the hybrid protein fully complements a *jnm1* null mutant at low temperature. If the staining pattern of the hybrid protein were due to aggregation or mislocalization, one might expect impaired *JNM1* function or some other defect. However, strains containing the hybrid protein in place of the wild-type Jnmlp grow at wild-type rates at low temperature and show no defects in nuclear migration or astral fiber morphology at 11°C.

Jnmlp May Play a Role in Tethering Astral Fibers in the Bud or May Be a Component of a Dynein Microtubule Motor

We envision a number of possible, but not necessarily exclusive, roles for Jnmlp. One attractive model is a role in anchoring astral microtubules to an attachment site in the bud. Jnmlp could associate with actin filaments in the bud, providing a link between actin and astral microtubules as proposed for yeast (Palmer et al., 1992) and metazoan embryos (Lutz et al., 1988; Hyman, 1989). The loss of a microtubule anchor could cause spindle misorientation and prevent nuclear migration. Microtubule tethering might also influence fiber length, again consistent with the elongated astral fibers observed in *jnm1* mutants at low temperature. As would be predicted for a tethering protein, the Jnmlp:β-galactosidase hybrid protein is primarily associated with the bud or near the bud. However, in many cells it is located close to the SPB and not at the tip of the astral fiber, as would be predicted.

Several recent observations lead us to favor the possibility that Jnmlp may be an auxiliary subunit for cytoplasmic dynein. A deletion in the dynein heavy chain gene (*dhc1/dyn1*) has a phenotype very similar to *jnm1* (Eshel et al., 1993; Li et al., 1993). Mutations in *dhc1/dyn1*, like *jnm1*, have a moderate defect in nuclear migration at 30°C which is greatly exacerbated at 11°C. At 11°C, both mutants have long, winding astral microtubules. *dhc1/dyn1* mutants, like *jnm1* mutants, exhibit no defects in karyogamy or chromosome segregation (Li et al., 1993). Double mutants between *jnm1* and *dhc1/dyn1* have a similar phenotype to either *dhc1* or *jnm1* alone (Yeh, E., and J. McMillan, unpublished observations). The lack of synergism between *jnm1* and *dhc1/dyn1* mutants is strong evidence that both genes are involved in the same process and would be predicted if Jnmlp and the dynein heavy chain are essential subunits of the same protein complex. A genetic screen to uncover mutations that are lethal in combination with *cin8*, which encodes a kinesin-like protein (Hoyt et al., 1992; Roof et al., 1992), has turned up a mutant allele of *jnm1* and multiple alleles of *dhc1/dyn1* (M. A. Hoyt, personal communication). This result provides additional evidence that the dynein heavy chain and Jnmlp are part of the same complex. Although both cytoplasmic and axonemal dynein are composed of multiple subunits, the sequence is only known for the largest (Gibbons et al., 1991; Ogawa, 1991) and one intermediate subunit of cytoplasmic dynein (Paschal et al., 1992). It is possible that Jnmlp is one of the additional subunits.

The location of the Jnmlp:β-galactosidase hybrid protein near the SPB or astral microtubules in the bud supports the model that Jnmlp has a role with a dynein-based motor required for spindle migration. Cytoplasmic dynein from other systems has been shown to be a minus end-directed motor (Paschal and Vallee, 1987; Schnapp and Reese, 1989; Schroer et al., 1989). If yeast dynein is also a minus end-directed motor and Jnmlp associates with dynein, Jnmlp would be expected to be located on the astral fiber. This location would allow the motor to pull the SPB towards the bud. In a significant number of cases, however, the Jnmlp:β-galactosidase hybrid is at or near the SPB. One could account for this result by proposing that the dynein motor could break from its anchor and run down the astral fiber to the SPB. It is also possible that yeast dynein has plus end-directed motor activity. Although purified dynein has minus end activity, there is pharmacological evidence that dynein-like motors may have both plus and minus end-directed activity (Schliwa et al., 1991). If Jnmlp were involved with a plus end-directed motor it would be expected to be associated with the SPB. As discussed above, we observe two distinct abnormal phenotypes for *jnm1* mutants, large budded cells with a single mislocalized nucleus and binucleate cells, suggesting that Jnmlp may have two independent roles. The variable location of Jnmlp:β-galactosidase could therefore reflect these separate roles.

We emphasize that neither *JNM1* nor *DHC/DYN1* are essential genes. At 30°C mutants with deletions in both genes grow with normal doubling times. This suggests that dynein is redundant with another mechanochemical system, either another dynein-like motor, which has not been uncovered by PCR or cross-hybridization, or an unrelated motor system. Mutations in *cin8*, a kinesin-related motor gene, have recently been shown to be lethal in combination with *jnm1* or *dhc1/dyn1* (Hoyt, M. A., D. Eshel, I. R. Gibbons, and W. S. Saunders, personal communication). This could indicate that the *CIN8*-encoded kinesin, which has been shown to have an important role in spindle elongation (Hoyt et al., 1992; Roof et al., 1992), also has a role that overlaps with that of dynein. It remains to be determined if this role is spindle orientation and migration.

We thank John Cooper (Washington University, St. Louis, MO) for providing us with anti-microtubule antibodies, helpful discussion and critically reading the manuscript; and Elain Yeh and Kerry Bloom (University of North Carolina, Chapel Hill, NC) for providing the YAC clone for the chromosome loss assay and helpful discussion, John Pringle (University of North Carolina, Chapel Hill, NC) for helpful discussion; and Tim Petty, Catherine Varner (North Carolina State University, Raleigh, NC), and Lucy Robinson (Louisiana State University Medical School, Shreveport, LA) for reading the manuscript. We also thank Andy Hoyt (Johns Hopkins University, Baltimore, MD), Dan Eshel (Brooklyn College, Brooklyn,

NY), Elaine Yeh and Kerry Bloom for sharing their data prior to publication.

This work was supported by National Institutes of Health grant GM47789.

Received for publication 28 October 1993 and in revised form 20 January 1994.

References

Becker, D. M., and L. Guarente. 1991. High-efficiency transformation of yeast by electroporation. *Methods Enzymol.* 194:182–187.

Berlin, V., C. A. Styles, and G. R. Fink. 1990. BIK1, a protein required for microtubule function during mating and mitosis in *Saccharomyces cerevisiae*, colocalizes with tubulin. *J. Cell Biol.* 111:2573–2586.

Cannon, J. F., and K. T. Tatchell. 1987. Characterization of *Saccharomyces cerevisiae* genes encoding subunits of cyclic AMP-dependent protein kinase. *Mol. Cell Biol.* 7:2653–2663.

Costigan, C., S. Gehrung, and M. Snyder. 1992. A synthetic lethal screen identifies SLK1, a novel protein kinase homolog implicated in yeast cell morphologies and cell growth. *Mol. Cell Biol.* 12:1162–1178.

Elledge, S. J., and R. W. Davis. 1988. A family of versatile centromeric vectors designed for use in the sectoring-shuffle mutagenesis assay in *Saccharomyces cerevisiae*. *Gene (Amst.).* 70:303–312.

Eshel, D., L. A. Urrestarazu, S. Vissers, J.-C. Jauniaux, J. C. van Vliet-Reedijk, R. J. Planta, and I. R. Gibbons. 1993. Cytoplasmic dynein is required for normal nuclear segregation in yeast. *Proc. Natl. Acad. Sci. USA.* 90:11172–11176.

Gerring, S. L., F. Spencer, and P. Hieter. 1990. The *CHL1 (CTF1)* gene product of *Saccharomyces cerevisiae* is important for chromosome transmission and normal cell cycle progression in G2/M. *EMBO (Eur. Mol. Biol. Organ.) J.* 9:4347-4358.

Gibbons, I. R., B. H. Gibbons, G. Mocz, and D. J. Asai. 1991. Multiple nucleotide-binding sites in the sequence of dynein beta heavy chain. *Nature (Lond.).* 352:640–643.

Gietz, D., A. St. Jean, R. A. Woods, and R. H. Schiestl. 1992. Improved method for high efficiency transformation of intact yeast cells. *Nucleic Acids Res.* 20:1425.

Goldring, E. S., L. I. Grossman, D. Krupnick, D. R. Cryer, and J. Marmur. 1970. The petite mutation in yeast: loss of mitochondrial deoxyribonucleic acid during induction of petites with ethidium bromide. *J. Mol. Biol.* 52:323–335.

Hieter, P., C. Mann, M. Snyder, and R. W. Davis. 1985. Mitotic stability of yeast chromosomes: a colony color assay that measures nondisjunction and chromosome loss. *Cell.* 40:381–392.

Hoyt, M. A., L. Totis, and B. T. Roberts. 1991. *S. cerevisiae* genes required for cell cycle arrest in response to loss of microtubule function. *Cell.* 66:507–517.

Hoyt, M. A., L. He, K. K. Loo, and W. S. Saunders. 1992. Two *Saccharomyces cerevisiae* kinesin-related gene products required for mitotic spindle assembly. *J. Cell Biol.* 118:109–120.

Huffaker, T. C., J. H. Thomas, and D. Botstein. 1988. Diverse effects of β-tubulin mutations on microtubule formation and function. *J. Cell Biol.* 106:1997–2010.

Hyman, A. A. 1989. Centrosome movement in the early divisions of *Caenorhabditis elegans*: a cortical site determining centrosome position. *J. Cell Biol.* 105:2123–2135.

Ito, H., Y. Fukuda, D. Murata, and A. Kimura. 1983. Transformation of intact yeast cells treated with alkali cations. *J. Bacteriol.* 153:163–168.

Jacobs, C. W., A. E. M. Adams, P. J. Szaniszlo, and J. R. Pringle. 1988. Functions of microtubules in the *Saccharomyces cerevisiae* cell cycle. *J. Cell Biol.* 107:1409–1426.

Kinoshita, N., M. Goebl, and M. Yanagida. 1991. The Fission Yeast *dis3*$^+$ gene encodes a 100-kDa essential protein implicated in mitotic control. *Mol. Cell Biol.* 11:5839–5847.

Kormanec, J., I. Schaaff-Gerstenschlager, F. K. Zimmermann, D. Perecko, and H. Kuntzel. 1991. Nuclear migration in *Saccharomyces cerevisiae* is controlled by the highly repetitive 313 kDa NUM1 protein. *Mol. Gen. Genet.* 230:277–287.

Lea, D. E., and C. A. Coulson. 1949. The distribution of the numbers of mutants in bacterial populations. *J. Genet.* 49:264–285.

Li, R., and A. W. Murray. 1991. Feedback control of mitosis in budding yeast. *Cell.* 66:519–531.

Li, Y.-Y., E. Yeh, T. Hays, and K. Bloom. 1993. Disruption of mitotic spindle orientation in a yeast dynein mutant. *Proc. Natl. Acad. Sci. USA.* 90: 10096–10100.

Lillie, S. H., and S. S. Brown. 1992. Suppression of a myosin defect by a kinesin-related gene. *Nature (Lond.).* 356:358–361.

Lupas, A., M. Van Dyke, and J. Stock. 1991. Predicting coiled coils from protein sequences. *Science (Wash. DC).* 252:1162–1164.

Lutz, D. A., Y. Hamaguchi, and S. Inoue. 1988. Micromanipulation studies of the asymmetric positioning of the maturation spindle in *Charptopterus* sp. oocytes: anchorage of the spindle to the cortex and migration of a displaced spindle. *Cell Motil. Cytoskeleton.* 11:83–96.

McConnell, S. J., and M. P. Yaffe. 1992. Nuclear and mitochondrial inheritance in yeast depends on novel cytoplasmic structures defined by the MDM1 protein. *J. Cell Biol.* 118:385–395.

Meluh, P. B., and M. D. Rose. 1990. *KAR3*, a kinesin-related gene required for yeast nuclear fusion. *Cell.* 60:1029–1041.

Myers, A. M., A. Tzagoloff, D. M. Kinney, and C. J. Lusty. 1986. Yeast shuttle and integrative vectors with multiple cloning sites suitable for construction of *lacZ* fusions. *Gene (Amst.).* 45:299–310.

Ogawa, K. 1991. Four ATP-binding sites in the midregion of the beta heavy chain of dynein. *Nature (Lond.).* 352:643–645.

Palmer, R. E., D. S. Sullivan, T. Huffaker, and D. Koshland. 1992. Role of astral microtubules and actin in spindle orientation and migration in the budding yeast, *Saccharomyces cerevisiae*. *J. Cell Biol.* 119:583–593.

Paschal, B. M., and R. B. Vallee. 1987. Retrograde transport by the microtubule-associated protein MAP 1C. *Nature (Lond.).* 330:181–183.

Paschal, B. M., A. Mikami, K. K. Pfister, and R. B. Vallee. 1992. Homology of the 74-kD cytoplasmic dynein subunit with a flagellar dynein polypeptide suggests an intracellular targeting function. *J. Cell Biol.* 118:1133–1143.

Perkins, D. D. 1949. Biochemical mutants of the smut fungus *Ustilago maydis*. *Genetics.* 34:607–629.

Pfarr, C. M., M. Coue, P. M. Grissom, T. S. Hays, M. E. Porter, and J. R. McIntosh. 1990. Cytoplasmic dynein is localized to kinetochores during mitosis. *Nature (Lond.).* 345:263–265.

Pringle, J. R., and L. H. Hartwell. 1981. The *Saccharomyces cerevisiae* cell cycle. *In* The Molecular Biology of the Yeast *Saccharomyces cerevisiae*. Vol. 1. Strathern, J. N., E. W. Jones, and J. R. Broach, editors. Cold Spring Harbor Laboratory, Cold Spring Harbor, NY. 97–142.

Pringle, J. R., A. E. M. Adams, D. G. Drubin, and B. K. Haarer. 1991. Immunofluorescence methods for yeast. *Methods Enzymol.* 194:565–608.

Roof, D. M., P. B. Meluh, and M. D. Rose. 1992. Kinesin-related proteins required for assembly of the mitotic spindle. *J. Cell Biol.* 118:95–108.

Rose, M. D., F. Winston, and P. Hieter. 1990. Methods in Yeast Genetics: A Laboratory Course Manual. Cold Spring Harbor Laboratory Press, Cold Spring Harbor, NY. 198 pp.

Rothstein, R. J. 1983. One-step gene disruption in yeast. *Methods Enzymol.* 101:202–210.

Sambrook, J., E. F. Fritsch, and T. Maniatis. 1989. Molecular Cloning: A Laboratory Manual. Cold Spring Harbor Laboratory Press, Cold Spring Harbor, NY. 545 pp.

Schatz, P. J., F. Solomon, and D. Bostein. 1988. Isolation and characterization of conditional-lethal mutations in the *TUB1* α-tubulin gene of the yeast *Saccharomyces cerevisiae*. *Genetics.* 120:681–695.

Schliwa, M., T. Shimizu, R. D. Vale, and U. Euteneuer. 1991. Nucleotide specificities of anterograde and retrograde organelle transport in *Reticulomyxa* are indistinguishable. *J. Cell Biol.* 112:1199–1203.

Schnapp, B. J., and T. S. Reese. 1989. Dynein is the motor for retrograde transport of organelles. *Proc. Natl. Acad. Sci. USA.* 86:1548–1552.

Schroer, T. A., E. R. Steuer, and M. P. Sheetz. 1989. Cytoplasmic dynein is a minus end-directed motor for membranous organelles. *Cell.* 56:937–946.

Stearns, T., M. A. Hoyt, and D. Bostein. 1990. Yerast mutants sensitive to antimicrotubule drugs define three genes that affect microtubule function. *Genetics.* 124:251–262.

Steuer, E. R., L. Wordeman, T. A. Schroer, and M. P. Sheetz. 1990. Localization of cytoplasmic dynein to mitotic spindles and kinetochores. *Nature (Lond.).* 345:266–268.

Sullivan, D. S., and T. C. Huffaker. 1992. Astral microtubules are not required for anaphase B in *Saccharomyces cerevisiae*. *J. Cell Biol.* 119:379–388.

Sutton, A., D. Immanuel, and K. T. Arndt. 1991. The SIT4 protein phosphatase functions in late G1 for progression into S phase. *Mol. Cell Biol.* 11:2133–2148.

Ursic, D., and M. R. Culbertson. 1991. The yeast homolog to mouse *Tcp-1* affects microtubule-mediated processes. *Mol. Cell Biol.* 11:2629–2640.

Vallen, E. A., T. Y. Scherson, T. Roberts, K. van Zee, and M. D. Rose. 1992. Asymmetric mitotic segregation of the yeast spindle pole body. *Cell.* 69:505–515.

Watts, F. Z., G. Shiels, and E. Orr. 1987. The yeast *MYO1* gene encoding a myosin-like protein required for cell division. *EMBO (Eur. Mol. Biol. Organ.) J.* 6:3499–3505.

Wilson, R. B., A. A. Brenner, T. B. White, M. J. Engler, J. P. Gaughran, and K. Tatchell. 1991. The *Saccharomyces cerevisiae SRK1* gene, suppressor of *bcy1* and *ins1*, may be involved in protein phosphatase function. *Mol. Cell Biol.* 11:3369–3373.